

2-Imino-thiazolidin-4-one Derivatives as Potent, Orally Active S1P₁ Receptor Agonists[†]

Martin H. Bolli,* Stefan Abele, Christoph Binkert, Roberto Bravo, Stephan Buchmann, Daniel Bur, John Gatfield, Patrick Hess, Christopher Kohl, Céline Mangold, Boris Mathys, Katalin Menyhart, Claus Müller, Oliver Nayler, Michael Scherz, Gunther Schmidt, Virginie Sippel, Beat Steiner, Daniel Strasser, Alexander Treiber, and Thomas Weller

Drug Discovery Chemistry, Actelion Pharmaceuticals Ltd., Gewerbestrasse 16, CH-4123 Allschwil, Switzerland

Received February 11, 2010

Sphingosine-1-phosphate (S1P) is a widespread lysophospholipid which displays a wealth of biological effects. Extracellular S1P conveys its activity through five specific G-protein coupled receptors numbered S1P₁ through S1P₅. Agonists of the S1P₁ receptor block the egress of T-lymphocytes from thymus and lymphoid organs and hold promise for the oral treatment of autoimmune disorders. Here, we report on the discovery and detailed structure–activity relationships of a novel class of S1P₁ receptor agonists based on the 2-imino-thiazolidin-4-one scaffold. Compound **8bo** (ACT-128800) emerged from this series and is a potent, selective, and orally active S1P₁ receptor agonist selected for clinical development. In the rat, maximal reduction of circulating lymphocytes was reached at a dose of 3 mg/kg. The duration of lymphocyte sequestration was dose dependent. At a dose of 100 mg/kg, the effect on lymphocyte counts was fully reversible within less than 36 h. Pharmacokinetic investigation of **8bo** in beagle dogs suggests that the compound is suitable for once daily dosing in humans.

Introduction

Selective agonists of the sphingosine-1-phosphate-1 (S1P₁) receptor are of current therapeutic interest for their ability to halt the exit of lymphocytes from lymph nodes and other secondary lymphoid organs. This interruption of lymphocyte migration, without affecting cell types of the innate immune system (e.g., neutrophils or macrophages), and without affecting cellular reactivity of lymphocytes to antigen challenge, promises a new immunomodulatory therapeutic principle for a variety of autoimmune diseases.

Sphingosine-1-phosphate (S1P, Figure 1) is a lysophospholipid that mediates a wealth of biological effects via extracellular signaling through five distinct G-protein coupled receptors, numbered S1P₁ through S1P₅.^{1–6} While the S1P₁, S1P₂, and S1P₃ receptors are expressed ubiquitously, the S1P₅ receptor, for instance, is mainly found in brain tissue, in particular in oligodendrocytes. The S1P₁ receptor couples to G_{ai/o} only, and downstream signaling has been reported to be mediated by the rat sarcoma GTPase (Ras), mitogen-activated protein kinases (MAPK), extracellular signal-regulated kinases (ERK), phosphoinositide 3-kinases (PI3K), and other pathways. The other S1P receptors are promiscuous with respect to G-protein coupling and, in addition to G_{ai/o}, activate G_{12/13} and, in the case of S1P₂ and S1P₃, also G_{αq}.

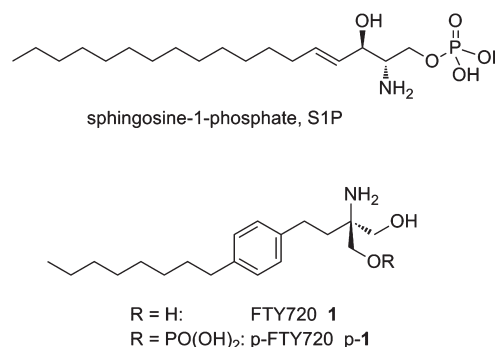


Figure 1. Structure of sphingosine-1-phosphate (S1P), FTY720 (**1**), and p-FTY720 (**p-1**).

S1P regulates many cellular functions by activating cell surface S1P receptors: effects on cell survival, proliferation, differentiation, apoptosis, adhesion, migration, and chemotaxis are all well-described.^{3,7–10} The actions of nonselective S1P receptor agonists have been described in detail for several tissues and organs such as the cardiovascular system,^{11–17} the lung,^{18,19} the cells of the immune system,^{20–22} the nervous system,^{23,24} and, most recently, bone tissue.²⁵ The observed effects include angiogenesis, endothelial barrier enhancement, airway and blood vessel constriction, alveolar epithelial barrier disruption, heart rate modulation, neurite extension, and bone homeostasis. It has been proven difficult to unambiguously assign these responses to one or more of the possible S1P receptor subtypes.

Attention has focused on selective S1P₁ receptor agonists. Selective S1P₁ receptor agonists have therapeutic potential to treat a variety of immune-mediated diseases such as multiple sclerosis, psoriasis, rheumatoid arthritis, or graft versus host

[†]This manuscript includes four X-ray crystallographic structures. The corresponding data sets have been deposited at the Cambridge Crystallographic Data Centre, 12 Union Road, Cambridge, CB2 1EZ, United Kingdom, <http://www.ccdc.cam.ac.uk/>, under the following ID numbers: compound **2**, CCDC 7711347; compound **5b**, CCDC 771348; compound **8g**, CCDC 771349; compound **8e**, CCDC 771350.

*To whom correspondence should be addressed. Phone: +41 61 565 65 70. Fax: +41 61 565 65 00. E-mail: martin.bolli@actelion.com.

disease. Many cells, in particular cells of the immune system, are able to migrate along a gradient of S1P by means of the S1P–S1P₁ receptor signaling axis.^{3,26,27} S1P₁ agonists interrupt lymphocyte migration and recruitment to sites of inflammation by sequestering the lymphocytes from blood circulation to lymphoid organs. This became evident when it was discovered that FTY720 (**1**, Figure 1), a compound which has long been known to sequester lymphocytes from circulating blood to lymphoid tissue,^{28–31} is phosphorylated *in vivo* to become a potent agonist (p-FTY720, p-**1**, Figure 1) at all S1P receptors except for S1P₂.^{32–35} Experiments with S1P₁ receptor knockout mice^{36,37} as well as S1P₁ selective agonists such as compound **1** analogues³⁸ or 5-(4-phenyl-5-(trifluoromethyl)-thiophen-2-yl)-3-(3-(trifluoromethyl)phenyl)-1,2,4-oxadiazole (SEW2871)^{39,40} have demonstrated that targeting S1P₁ is sufficient to cause lymphocyte sequestration to lymphoid organs.

To explain the lymphocyte sequestration observed with compound **1** and other S1P agonists,^{39–41} two hypotheses have been proposed. In the “functional antagonist” hypothesis, the S1P concentration gradient⁴² that exists between blood plasma and lymph was proposed as a driving force for T-lymphocytes (in contrast to B-cells⁴³) to exit the lymph nodes and re-enter systemic circulation.^{44–46} The activation of the S1P₁ receptor is thought to lead to receptor internalization and thus desensitization of the cell toward an external S1P gradient. The second hypothesis claims the tightening of the lymphatic endothelial cell junctions as the main reason for the lymphocytes’ inability to leave the lymphoid tissue.^{13,34,40,41,47,48} An intriguing characteristic of the immunomodulation achieved with S1P₁ agonists is the fact that lymphocytes, although hindered in their ability to travel through the body, survive and are still able to react to an intruding microbial insult.^{30,49,50} Recent studies have shown that a low dose of compound **1** may even enhance clearance of a chronic viral infection.⁵¹

In clinical trials, compound **1** has shown great promise in the treatment of multiple sclerosis patients.^{52–54} Results obtained in preclinical experiments suggest that compound **1** slows down disease progression not only by blocking T cell migration to the central nervous system but also by directly affecting brain cells such as astrocytes and oligodendrocytes. S1P mediated activation of astrocytes and glial cells may trigger endogenous repair mechanisms and support survival of neural cells.^{55–60}

Activation of the S1P₃ pathway has been reported to cause heart rate reduction,^{61–64} vaso- and bronchoconstriction, and pulmonary epithelial leakage.⁶⁵ In the context of an immunomodulating drug, agonistic activity on S1P₃ is therefore deemed undesirable.

An overwhelming number of patents claiming novel selective S1P₁ receptor agonists have been published in the past few years, and in addition to compound **1**, several molecules, e.g. KRP203 (Kyorin, Novartis), BAF312 (Novartis), CS-0777 (Daiichi Sankyo), and Ono-4641 (Ono Pharmaceutical Company), entered clinical trials.⁶⁶ Here we report on the discovery, synthesis, and detailed structure–activity relationships of a novel class of S1P₁ agonists which led to the selection of a compound suitable for clinical development.

High-throughput screening (HTS) of our in-house compound collection identified several iminothiazolidinone derivatives as S1P₁ receptor agonists (Figure 2). Compound **2** was the most potent representative in this hit cluster and showed an EC₅₀ of 200 nM on S1P₁ and of about 1 μ M on S1P₃. Thus,

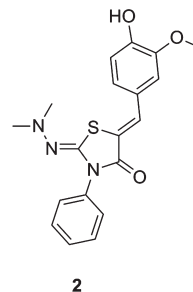


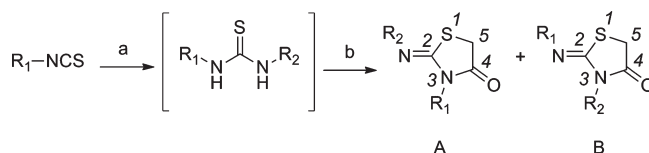
Figure 2. Structure of the high throughput screening hit.

the scaffold of compound **2** served as a starting point for further optimization of this class.

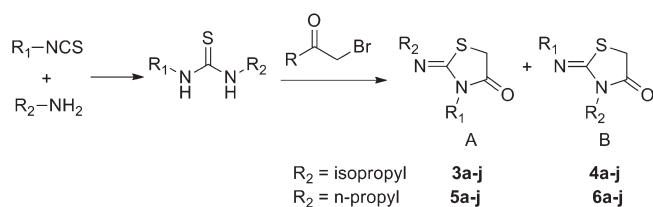
Chemistry

Several synthetic routes give access to substituted 2-iminothiazolidin-4-ones.^{67–73} The cyclization of substituted thioureas with a halo acetic acid derivative to form the corresponding 2-iminothiazolidin-4-one has been described almost one and a half centuries ago,^{74–76} albeit the structure of the isolated products was originally assigned, incorrectly, as 2-thiohydantoin. The correct constitution of the 2-iminothiazolidin-4-one, also known as pseudothiohydantoin, was first proposed by Liebermann et al. in 1879.^{77,78} The discussion on the tautomerism of this molecule continued for more than a century.⁷⁹ Today, commercial availability of a great variety of aryl and alkyl isothiocyanates gives easy access to thioureas and therefore makes the pathway in Scheme 1 very attractive for a rapid assembly of a large array of substituted 2-iminothiazolidin-4-one scaffolds. Thus, reacting an aryl or alkyl isothiocyanate with a primary amine furnished the corresponding thiourea derivative, which was directly cyclized to the iminothiazolidinone by treating this intermediate with a bromoacetic acid ester in the presence of pyridine. It is well-known that this synthetic route usually gives a mixture of the two isomeric 2-iminothiazolidin-4-ones of the general structures A and B.^{76,67} The regioselectivity of the cyclization is not only influenced by the reaction conditions (e.g., solvent, reaction temperature, presence or absence of a base)^{67,80} and the choice of the halo acetic acid derivative^{81–83} but also by the nature of the two substituents R₁ and R₂ of the thiourea intermediate. For example, it has been reported that under thermodynamic control the more electron withdrawing substituent of R₁ and R₂ usually ends up at N2 of the 2-imino-4-thiazolidinone.^{84,85} The regioselectivity issue is further complicated by the fact that 2-alkylimino-3-(hetero)aryl-4-thiazolidinones, which form under kinetic reaction control, isomerize to the corresponding thermodynamically more stable 2-(hetero)aryl-3-alkyl-4-thiazolidinones, for instance, when heated in alcoholic solutions, in particular in the presence of acids.^{67,80} In addition to these reports, we observed that steric effects

Scheme 1. Synthesis of the 2-Imino-thiazolidin-4-one Scaffold^a



^a(a) R₂-NH₂, MeOH, rt, 1–4 h; (b) ClCH₂COOMe, pyridine, rt, 16–24 h; or (a) R₂-NH₂, DCM, rt, 1–3 h; (b) BrCH₂COBr, pyridine, rt, 1–18 h.

Table 1. Regioselectivity of the 2-Imino-thiazolidin-4-one Scaffold Synthesis^a

R ₁	R	R ₂	x	isopropyl		n-propyl	
				OCH ₃ 3x:4x	Br 3x:4x	OCH ₃ 5x:6x	Br 5x:6x
phenyl	a			11:1 ^b	26:1	1:8	25:1
2-methyl-phenyl	b			4:1	42:1 ^k	1:10	41:1
3-methyl-phenyl	c			13:1	63:1	1:8	34:1
4-methyl-phenyl	d			18:1	54:1	1:7	28:1
2,6-dimethyl-phenyl	e			1:13 ^j	18:1	1:100 ^e	21:1 ^d
2-chloro-phenyl	f			3:1	47:1	1:24 ^e	47:1
2-methoxy-phenyl	g			10:1	49:1	1:6	22:1
3-pyridyl	h			5:3 ^f	59:1	1:73 ^j	29:1 ^j
cyclohexyl	i			1:2 ^g	1:1	1:100	2:1
benzyl	j			100:1 ⁱ	2:1 ^h	2:1 ^k	1:1 ^k

^a Regio-isomer ratios A:B as assessed by LC-MS run under acidic conditions (Zorbax SB-AQ column, see Experimental Section) at 230 nm; the following ratios have also been determined by ¹H NMR analysis of the crude reaction mixtures. ^b 10:1. ^c 1:42. ^d 15:1. ^e 1:19. ^f 5:3. ^g 1:2. ^h 5:2. ⁱ 100:1. ^j Ratio determined by ¹H NMR only. ^k Ratio determined using LC-MS run under basic conditions (Zorbax Extend C18 column, see Experimental Section).

also play an important role in this reaction. To illustrate our observations, the regioselectivity of some cyclization reactions carried out in the course of this study are compiled in Table 1.

When R₁ represents an unsubstituted or monosubstituted phenyl ring (compound series a–d, f, and g in Table 1), amines R₂-NH₂ branched at the α-position such as an isopropyl amine (but also a *tert*-butyl, a cyclopropyl, or an *N,N*-dimethylamino amine, see Experimental Section) furnished the desired isomers **3a–d,f,g** in good yields and gave only small amounts of the isomers **4a–d,f,g**. This is in strong contrast to the case wherein R₂ represents a straight alkyl chain such as an *n*-propyl group. In this case, the cyclization of the corresponding thioureas with methyl chloroacetate almost exclusively led to the formation of the undesired isomers **6a–d,f,g**. Hence, the second step had to be modified in order to reverse the product distribution in favor of isomers **5a–d,f,g**. Work by Pihlaja et al.^{81–83} suggested to employ the more reactive bromo acetyl bromide (Table 1, R = Br) instead of methyl bromoacetate. This established the isomers **5a–d,f,g** as the major product regardless of the nature of R₁ and R₂. In the case where R₂ represents an isopropyl group, the regioselectivity of the cyclization reaction using methyl bromoacetate was reduced for the two ortho-substituted phenyl groups (series b and f) and even reversed in favor of isomer **4e** in the 2,6-dimethylphenyl case (series e), indicating that steric effects influence the regioselectivity of the cyclization step. In the *n*-propyl series, the two ortho-substituted phenyl series e and f showed a strong preference for scaffold B, i.e., compounds **6e** and **6f**. Nevertheless, the use of bromoacetyl bromide in the cyclization step for both the isopropyl as well as the *n*-propyl series established the compounds **3b,e,f** and **5b,e,f**, respectively, as the prevailing isomer. The series wherein R₁ represents a 3-pyridyl residue (series h, Table 1) behaves very

similarly to the corresponding phenyl derivatives. Mechanistic considerations explaining these observations have been discussed in detail by Pihlaja et al.^{81–83}

The results obtained with the cyclohexyl (series i, Table 1) can be rationalized following analogous reasoning. In the series of 1-cyclohexyl-3-isopropyl thiourea, the two nitrogens bearing the cyclohexyl group and the isopropyl group are electronically and sterically similar, which results in an almost 1:1 distribution of the two cyclization products **3i** and **4i**. In the case of the 1-cyclohexyl-3-*n*-propyl thiourea, the *n*-propyl group is sterically less demanding and the cyclization therefore occurs in favor of the product **6i** when methyl bromoacetate is used as the cyclization reagent. However, when bromoacetyl bromide is employed, the comparable electronic nature⁸² rather than the steric environment of the thiourea nitrogens appears to dominate the outcome of the cyclization reaction and an almost 1:1 mixture of the two products **5i** and **6i** is obtained. In the benzyl series (**3–6j**), similar arguments may explain the regioselectivity of the cyclization reaction. The nitrogen bearing the benzyl group is more reactive than the one bearing the isopropyl group and reacts with the ester function of methyl bromoacetate to form isomer **3j**. In the case of 1-benzyl-3-*n*-propyl-urea, the two thiourea nitrogens display similar reactivities and an almost 1:1 mixture of **5j** and **6j** is obtained for both cyclization reagents.

In general, the 2-alkylimino-3-phenyl-thiazolidin-4-ones **3a–g** and **5a–g** can be separated from their isomeric 3-alkyl-2-phenylimino-thiazolidin-4-ones **4a–g** and **6a–g**, respectively, by a simple acid–base extraction. Under acidic conditions, the compounds **3a–g** and **5a–g** are extracted into the aqueous phase while the corresponding isomers **4a–g** and **6a–g** remain in the organic phase (diethyl ether). Hence, separation of the two phases separates the two isomers. The acidic aqueous phase is basified to enable extraction of the desired compounds **3a–g** and **5a–g** into diethyl ether or dichloromethane. This behavior is reflected in the different p*K*_a values of compounds of scaffold A and B. For instance, the experimentally determined p*K*_a value for compound **3a** is 4.1 while it is clearly below 2 for its isomer **4a**. In the case of the 2,3-dialkyl or the alkyl-benzyl substituted 2-imino-4-thiazolidinones, the extractive separation is not possible as both isomers have similar p*K*_a values. The separation is more challenging and can be effected by preparative (HPLC) chromatography. Analytically, the two isomers of structure A and B can be separated easily under LC-MS conditions (see Experimental Section), with isomer A often being clearly more polar than isomer B.

The ¹H NMR chemical shift of the C1-protons of the former primary alkyl-amine component is diagnostically useful to distinguish between the two isomers.⁸⁰ For isomer A, the α-protons of the 2-alkylimino-substituent appear in the range of 2.7–3.5 ppm. The corresponding protons of the 3-alkyl-substituent of isomer B are shifted toward the lower field by as much as 1.3 ppm. This assignment is corroborated by heteronuclear multiple bond correlation (HMBC) spectra⁸⁵ that were acquired for several pairs of isomer A and B. While in isomer B the α-protons of the 3-alkyl-substituent clearly coupled to both the carbons C2 and C4, the corresponding α-protons of the 2-alkylimino substituent in isomer A only showed coupling to C2 of the thiazolidinone scaffold (atom numbering see Scheme 1).

The structure of the compounds **5a–g** is further corroborated by an alternative synthesis. The pathway illustrated for

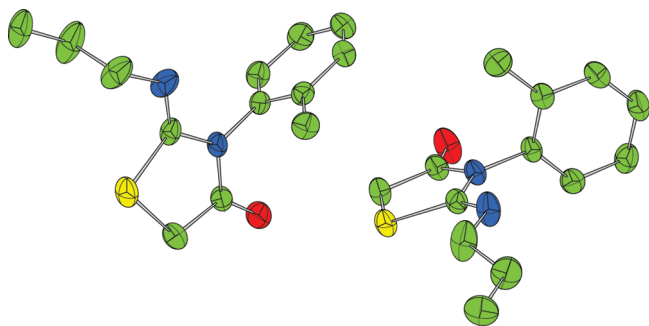
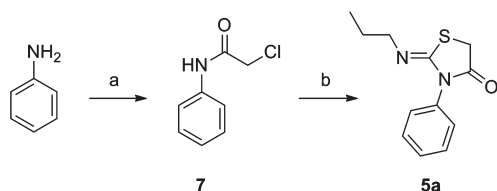


Figure 3. As determined by X-ray structure analysis, there are two atropisomers of compound **5b** in the asymmetric unit of single crystals of the compound. Anisotropic thermal ellipsoids are drawn at a 50% level. Hydrogen atoms have been omitted for reasons of clarity. For details, see the Experimental Section and Supporting Information.

Scheme 2. Alternative Synthesis of Scaffold **5a**^a



^a (a) ClCOCH₂Cl, DCM, Et₃N, −78 to 20°C, 3h; (b) NaH, *n*-propyl-NCS, rt, 4 h.

compound **5a** in Scheme 2^{86–88} establishes the structure of **5a** in an unambiguous fashion. In a first step, aniline is reacted with chloroacetic acid chloride to furnish 2-chloro-*N*-phenylacetamide **7**. This compound is then treated with *n*-propylisothiocyanate under basic conditions to presumably form 3-*n*-propyl-1-(2-chloro-acetyl)-1-phenyl-thiourea as an intermediate which immediately cyclizes to the desired 2-propylimino-3-phenylthiazolidin-4-one **5a** in acceptable yields. The product thus obtained is identical to the one isolated as isomer **A** from the synthesis shown in Scheme 1. Finally, the structural assignment, in particular the configuration of the exocyclic double bond, was confirmed by X-ray analysis of crystals of compound **5b**. Interestingly, there are two atropisomers^{89,90} present in the asymmetric unit of crystals of **5b** (Figure 3).

A wealth of conditions are known to effect the condensation of a 2-imino-4-thiazolidinone scaffold with an aliphatic or aromatic aldehyde to furnish the corresponding 5-alkylidene- or 5-arylidene 4-thiazolidinone.^{67,68} For this study, the condensation of substituted benzaldehydes was usually carried out in acetic acid in the presence of sodium acetate at temperatures ranging from 60 to 110 °C. For compounds **8bf** to **8bk** and **8bn** to **8bp**, the desired side chains at the 5-benzylidene-moiety were introduced by either condensing the appropriately substituted benzaldehyde or by elaborating these side chains in steps that followed the condensation reaction (for details, see Experimental Section and Supporting Information). Chromatographic behavior as well as ¹H NMR spectroscopic data of compounds **8** consistently showed the presence of only one configurational isomer in the material isolated from the condensation reaction (Scheme 3). The *Z,Z* configuration of these products was confirmed by X-ray analysis of crystals of compounds **2**, **8e** (see Supporting Information), and **8g** (Figure 4). The structure of all compounds **8** was therefore assigned to the *Z,Z*-isomer. Compounds bear-

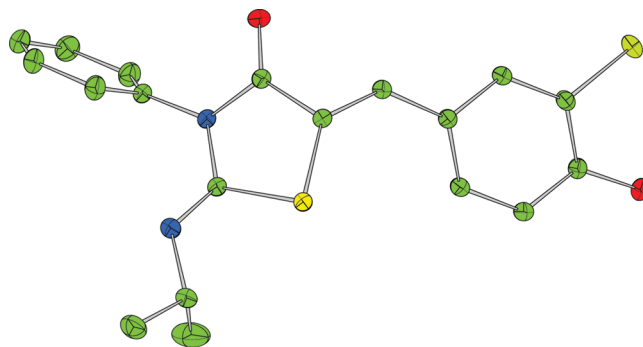
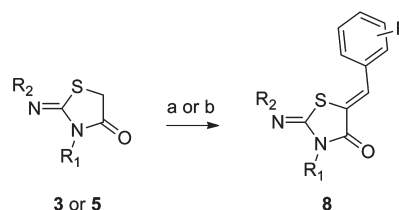


Figure 4. Molecular structure of compound **8g** as determined by X-ray structure analysis. Anisotropic thermal ellipsoids are drawn at a 50% level. Hydrogen atoms have been omitted for clarity reasons. For details, see the Experimental Section and Supporting Information.

Scheme 3^a

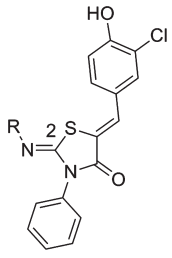


^a (a) 1–2 equiv substituted benzaldehyde, ethanol, piperidine, 80°C, 18 h; (b) 1–2 equiv substituted benzaldehyde, 2 equiv NaOAc, HOAc, 60–110°C, 3–24 h.

ing an ortho-substituted 3-phenyl-substituent (e.g., **8t**, **8z**, **8aa**, etc.), showed axial chirality due to hindered rotation around N3–C1(phenyl) bond in accordance with a recent report by Erol et al.⁸⁹ In the case of **8bo** (vide infra), the two atropisomers were separated by means of HPLC using a chiral stationary phase. A chloroform or methanol solution of the pure atropisomers re-equilibrated to the original 1:1 mixture within about one week at room temperature.

Structure–Activity Relationships in Vitro

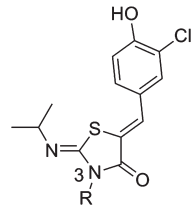
The following SARs of the 2- and 3-substituent at the iminothiazolidinone scaffold are illustrated with a series of compounds incorporating a 3-chloro-4-hydroxy-benzylidene substituent at position 5 of the iminothiazolidine scaffold, as this pattern generally afforded more potent compounds (e.g., **8a**) than the 4-hydroxy-3-methoxy-benzylidene substituent present in **2**. The compounds compiled in Table 2 illustrate the SAR of the 2-substituent of the core thiazolidinone. Starting from compound **8a**, first attempts aimed at replacing the hydrazone-type substructure by a presumably more benign (alkyl)-imine moiety. As illustrated by compound **8g**, this is indeed possible without loss of activity. In a second step, the chain length at the exocyclic imine (N2) was investigated. At a concentration of 10 μM, the compound lacking a substituent at this nitrogen (**8b**) showed only residual activity on the S1P₁ and S1P₃ receptor. With respect to potency on S1P₁, an *n*-propyl (**8e**) or an isopropyl chain (**8g**) at the exocyclic imine appear to be optimal. The potency optimum on the S1P₃ receptor is shifted toward the more bulky *sec*-butyl (**8h**) and *tert*-butyl (**8i**) chains. As a consequence, the S1P_{1/3} selectivity observed for compounds **8e** and **8g** is reversed for **8h** and **8i**. Cycloalkyl chains (as in **8j** to **8m**) did not bring any advantage over straight or branched open chains.

Table 2. SAR of the 2-Imino Substituent^a


compd	R	S1P ₁		S1P ₃	
		EC ₅₀ [nM]	σ_g	EC ₅₀ [nM]	σ_g
8a	dimethylamino	62	1.36	140	1.35
8b	hydrogen	> 10000		> 10000	
8c	methyl	990	1.47	8810	1.20
8d	ethyl	186	1.08	1229	1.20
8e	<i>n</i> -propyl	67	1.64	189	1.29
8f	<i>n</i> -butyl	112	1.21	264	1.31
8g	isopropyl	47	1.35	120	1.23
8h	(<i>rac</i>)- <i>sec</i> -butyl	102	1.36	59	1.18
8i	<i>tert</i> -butyl	147	1.20	96	1.36
8j	cyclopropyl	103	1.66	114	1.13
8k	cyclobutyl	202	1.63	128	1.13
8l	cyclopentyl	347	1.32	302	1.42
8m	cyclohexyl	584	1.13	310	1.26

^a EC₅₀ values for compounds **8** as determined in a GTPγS assay using membrane preparations of CHO cells overexpressing the human S1P₁ and S1P₃ receptor, respectively. Data are given as geometric mean and geometric standard deviation (σ_g) of at least three independent measurements.

To illustrate the SAR of the N3 substituent, a selection of compounds, wherein the 2-isopropylimino and the 5-(3-chloro-4-hydroxy-benzylidene) substituent of the core thiazolidinone are kept constant, is listed in Table 3. For the following discussion, the iminothiazolidinone **8g** featuring an unsubstituted phenyl ring at N3 shall serve as a reference compound. Compared to this reference, the isopropyl derivative **8n** shows almost identical potency on S1P₁ and S1P₃. Interestingly, the allyl compound **8s** displays an almost identical affinity for S1P₁ but is significantly less potent on S1P₃. The *n*-hexyl derivative **8o**, on the other hand, is equally potent on S1P₃ but has a reduced affinity for the S1P₁ receptor. Compound **8q** featuring a six-atom chain incorporating an ester functionality has a similar affinity profile as **8o**. However, if the ester function in **8q** is hydrolyzed to give the corresponding acid **8r**, the affinity for both the S1P₁ and S1P₃ receptor is lost. The compound with a cyclohexyl substituent at N3 (**8p**) is clearly more potent on S1P₁ and S1P₃ when compared to the phenyl analogue **8g**. The compounds **8t** to **8ah** illustrate the rather shallow SAR of the substitution pattern at the N3-phenyl moiety. In general, one or two methyl groups, a chlorine, or chlorine combined with a methyl group or a substituent in the 2- and/or 3-position of the phenyl ring lead to potency profiles similar to the one of the unsubstituted analogue **8g**. Ethyl and methoxy groups attached to the phenyl ring gave less potent compounds. The selectivity for the S1P₁ receptor is most pronounced for compounds bearing a 2-substituent (e.g., **8t**, **8aa**, **8ae**). This selectivity is reduced for the corresponding 3-substituted analogues (e.g., **8u**, **8ab**, **8af**). Compounds bearing a 4-substituent are the least selective within a given series and represent, although less potent, balanced dual S1P_{1/3} (e.g., **8v**) or even slightly S1P₃ selective (**8ag**) receptor

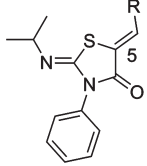
Table 3. SAR of the 3-Substituent^a


compd	R	S1P ₁		S1P ₃	
		EC ₅₀ [nM]	σ_g	EC ₅₀ [nM]	σ_g
8n	<i>iso</i> -propyl	58	1.32	162	1.11
8o	<i>n</i> -hexyl	282	1.04	118	1.12
8p	cyclohexyl	10	1.19	18	1.09
8q	ethoxycarbonyl-ethyl	479	1.15	125	1.19
8r	carboxyethyl	> 10000		> 10000	
8s	allyl	55	1.60	821	1.16
8g	phenyl	47	1.35	120	1.23
8t	2-methyl-phenyl	34	1.43	139	1.45
8u	3-methyl-phenyl	110	1.22	200	1.31
8v	4-methyl-phenyl	78	2.01	88	1.56
8w	2,6-dimethyl-phenyl	154	1.33	307	1.18
8x	2,3-dimethyl-phenyl	72	1.15	350	1.60
8y	2,4-dimethyl-phenyl	179	1.26	458	1.36
8z	2-ethyl-phenyl	124	1.34	335	1.39
8aa	2-chloro-phenyl	54	1.49	425	2.10
8ab	3-chloro-phenyl	35	1.53	129	1.06
8ac	3-chloro-2-methyl-phenyl	31	1.36	246	1.26
8ad	3-chloro-4-methyl-phenyl	47	1.48	144	1.29
8ae	2-methoxy-phenyl	106	1.17	428	1.64
8af	3-methoxy-phenyl	259	1.45	514	1.08
8ag	4-methoxy-phenyl	251	1.59	127	1.13
8ah	2,4-dimethoxy-phenyl	875	1.73	525	1.26
8ai	3-pyridyl	356	2.05	228	1.03
8aj	benzyl	630	1.30	674	1.12
8ak	phenethyl	925	1.30	183	1.42
8al	4-phenyl-butyl	1815	1.08	212	1.13

^a EC₅₀ values for compounds **8** determined as described for Table 2.

agonists. Replacing the phenyl substituent in **8g** by a 3-pyridine ring (compound **8ai**) reduced the compound's potency, in particular on the S1P₁ receptor. Similarly, moving the phenyl ring further away from N3 as exemplified by the benzyl (**8aj**), the phenethyl (**8ak**), and the 4-phenyl-butyl (**8al**) derivatives significantly reduced the compound's affinity for the S1P₁ receptor.

We then turned our attention to optimizing the benzylidene substituent in position 5 of the core iminothiazolidinone. The compounds compiled in Tables 4 and 5 illustrate that the S1P₁ receptor is generally more susceptible to changes in the nature and position of substituents at the 5-benzylidene moiety. Compounds wherein R (Table 4) represents an alkyl (e.g., ethyl, isopropyl) or a cycloalkyl (e.g., cyclopropyl, cyclohexyl) group did not show any activity on the S1P₁ receptor (data not shown). Compound **8am** with an unsubstituted benzylidene substituent at position 5 showed only weak activity on S1P₁ and moderate activity on S1P₃. For the following discussion, the 4-hydroxy-3-chloro-benzylidene derivative **8g** shall again serve as a reference compound. Compounds **8an** to **8aq** illustrate the effect of a 3-substituent next to the 4-hydroxy group of the benzylidene moiety in **8g**. A chloro or a methyl substituent clearly improve the compound's potency on S1P₁ and, in the case of the methyl group, also on S1P₃. The

Table 4. SAR of 5-Benzylidene Substituent^a


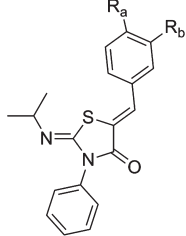
compd	R	S1P ₁		S1P ₃	
		EC ₅₀ [nM]	σ _g	EC ₅₀ [nM]	σ _g
8am	phenyl	1237	1.23	317	1.02
8an	4-hydroxy-phenyl	122	1.52	95	1.09
8ao	4-hydroxy-3-fluoro-phenyl	225	1.07	99	1.36
8g	4-hydroxy-3-chloro-phenyl	47	1.35	120	1.23
8ap	4-hydroxy-3-methyl-phenyl	37	1.46	50	1.49
8aq	4-hydroxy-3-methoxy-phenyl	200	1.95	335	2.12
8ar	4-methoxy-phenyl	201	1.32	106	1.27
8as	3,4-dimethoxy-phenyl	224	1.17	1385	1.87
8at	4-dimethylamino-phenyl	148	2.03	165	1.63
8au	4-bromo-phenyl	1038	1.09	136	1.76
8av	3-methoxy-phenyl	185	1.39	35	1.10
8aw	3-hydroxy-phenyl	752	1.55	103	1.02
8ax	3-hydroxy-4-methoxy-phenyl	444	2.35	212	1.56
8ay	3,4-dihydroxy-phenyl	> 10000		> 10000	
8az	2-methyl-phenyl	6452	1.43	5791	1.49
8ba	2-chloro-phenyl	> 10000		2583	1.21
8bb	2-methoxy-phenyl	> 10000		6689	1.42

^a EC₅₀ values for compounds **8** determined as described for Table 2.

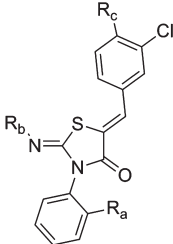
methoxy group in **8aq**, however, reduces the compound's affinity for both S1P receptors.

As exemplified by the two compounds **8ar** and **8as**, replacing the 4-hydroxy substituent of **8an** and **8aq**, respectively, by a 4-methoxy group does not improve the compounds' affinity for the two S1P receptors. In fact, the 3,4-dimethoxy-phenyl derivative **8as** is clearly less active on S1P₃ when compared to its 4-hydroxy-3-methoxy analogue **8aq**. Replacing the 4-hydroxy group in **8an** by a 4-dimethylamino group yields compound **8at**, which shows an almost identical affinity profile. A clear loss of affinity for the S1P₁ receptor is seen when the 4-hydroxy group in **8an** is replaced by a bromine atom (**8au**). Removing the 4-hydroxy substituent in **8aq** while keeping the 3-methoxy group to give compound **8av** has no effect on S1P₁ affinity but improves the compound's ability to activate the S1P₃ receptor by about 1 order of magnitude. In contrast to the 4-substituted series, converting the 3-methoxy group in **8av** to a 3-hydroxy group (compound **8aw**) results in a significant loss of affinity for both receptors. As shown with compound **8ax**, the affinity can be restored partially by adding a 4-methoxy substituent. Incorporating a 4-hydroxy substituent to compound **8aw**, however, is detrimental for the compound's S1P agonistic activity (compound **8ay**). As illustrated by the three compounds **8az**, **8ba**, and **8bb**, a 2-substituent at the phenyl ring significantly hampers the compound's affinity for the S1P₁ and S1P₃ receptor.

A last group of compounds shall illustrate the SAR of a number of polar chains that have been attached to the 5-benzylidene substituent. As compared to the phenol **8an**,

Table 5. SAR of the para-Substituent at the 5-Benzylidene Moiety^a


Compound	R _a	R _b	S1P ₁		S1P ₃	
			EC ₅₀ [nM]	σ _g	EC ₅₀ [nM]	σ _g
8an	OH	H	122	1.52	95	1.09
8bc		H	408	1.41	86	1.23
8bd		H	102	1.36	59	1.18
8be		H	98	1.81	54	1.29
8bf		H	95	1.93	114	1.19
8bg		H	58	1.11	68	1.86
8bh		H	143	1.36	240	1.09
8bi		H	8631	1.23	1430	1.03
8bj	H		1414	1.06	531	1.37
8bk		H	343	1.20	114	1.75

^a EC₅₀ values for compounds **8** determined as described for Table 2.**Table 6.** EC₅₀ Values of Compounds **8** Combining Optimized Substituents^a


Compound	R _a	R _b	R _c	S1P ₁		S1P ₃	
				EC ₅₀ [nM]	σ _g	EC ₅₀ [nM]	σ _g
8g	H	isopropyl	OH	47	1.35	120	1.23
8bl	methyl	n-propyl	OH	19	1.21	81	1.26
8bm	methyl	n-propyl		11	1.11	124	1.17
8bn	methyl	n-propyl		12	1.23	174	1.34
8bo	methyl	n-propyl		9.1	1.34	123	1.43
8bp	methyl	n-propyl		9.7	1.28	109	1.24

^a EC₅₀ values for compounds **8** determined as described for Table 2.

the corresponding hydroxymethyl substituted derivative **8bc** is less potent on S1P₁. Interestingly, the activity on S1P₁ is restored when the alcohol function is moved further away

from the phenyl ring by either an alkyl (as in **8bd** and **8be**) or an alkoxy linker (as in **8bf** and **8bg**). In fact, when compared to **8an**, the hydroxy-propoxy substituent in **8bg** even slightly improves the compound's affinity for the S1P₁ receptor. On the other hand, there is a weak trend for an increasing chain length to steadily improve the compound's affinity for the S1P₃ receptor. While the glycerol derivative **8bh** shows an affinity for the S1P₁ receptor, which is comparable to the one of the phenol **8an**, its isomer **8bi** is considerably less active on both S1P receptors. Compound **8bj** highlights the importance of the correct attachment point of a hydroxy-alkyl side chain.

With respect to potency on the S1P₁ receptor and selectivity against S1P₃, the one-dimensional SAR studies discussed above can be summarized as follows: at the exocyclic imine nitrogen (N2), an isopropyl or an *n*-propyl chain appears to be optimal (Table 2). At N3, a 2- and/or a 3-substituted phenyl ring substituted with either a methyl group or a chlorine atom gave best compounds (Table 3). A 3-chloro or 3-methyl substituent in combination with an hydroxy, an hydroxyalkyl, or a mono- or dihydroxyalkoxy group in position 4 of the benzylidene moiety gave most attractive examples (Tables 4 and 5). With these data at hand, we set out to prepare an array of compounds wherein the substitution patterns found to be optimal in these individual one-dimensional SAR studies were combined. As illustrated by compounds **8bl** to **8bn** (Table 6), combining these substituents indeed led to compounds of superior potency on the S1P₁ receptor.

Table 7. Effect on Blood Lymphocyte Counts after Oral Administration of Selected Compounds **8**^a

compd	lymphocyte counts				
	absolute [10 ⁹ cells/L]		relative [% of <i>t</i> = 0 h]		
	0 h	3 h	6 h	24 h	interpretation
vehicle	7.5 ± 0.2	3.5 ± 2	2 ± 3	15 ± 3	
8g	6.9 ± 0.4	−16 ± 4	−15 ± 8	−9 ± 4	inactive
8bl	6.9 ± 0.5	29 ± 7	24 ± 7	40 ± 8	inactive
8bm	6.9 ± 0.4	−54 ± 4	−38 ± 5	28 ± 3	active
8bn	9.3 ± 0.4	−67 ± 3	−71 ± 1	19 ± 4	active
8bo	7.0 ± 0.4	−65 ± 4	−63 ± 3	−18 ± 8	active
8bp	7.9 ± 0.4	−64 ± 2	−55 ± 3	15 ± 7	active

^a Relative blood lymphocyte count changes ± SEM 3, 6, and 24 h after oral administration of vehicle (*n* = 30) or 10 mg/kg of a compound **8** (*n* = 6) to male Wistar rats, as compared to absolute lymphocyte counts before compound administration (*t* = 0 h).

Table 8. DMPK Data of Selected Compounds **8**^a

compd	intrinsic clearance						pharmacokinetic parameters				
	liver microsomes [μL/min × mg protein]			hepatocytes [μL/min × 10 ⁶ cells]			<i>F</i> [%]	<i>C</i> _{max} (dose) ng/mL (mg/kg)	<i>t</i> _{1/2} [h]	clearance [mL/min/kg]	<i>V</i> _{ss} [L/kg]
	rat	dog	human	rat	dog						
8g	67	nd	<4	nd	nd	nd	nd	nd	nd	nd	nd
8t ^b	158	nd	27	19.8	nd	<1%	11 (10)	0.7	105	3.0	
8bl	229	nd	7	nd	nd	<1%	8.1 (3)	0.2	92	1.1	
8bf ^b	4	nd	4	12	nd	72	499 (10)	2.0	32	4.0	
8bm	166	nd	<4	nd	nd	23	129 (3)	1.4	48	5.2	
8bn ^b	27	nd	4	9.1	nd	90	311 (10)	1.6	41	5.6	
8bo	56	7	4	3.7	1.0	35	409 (3)	1.3	25	3.3	
						69 ^c	1360 (3) ^c	10 ^c	1.3 ^c	0.9 ^c	

^a After oral and intravenous administration of the compounds **8** to male Wistar rats (*n* = 3) at 3 and 0.3 mg/kg, respectively. ^b Oral dose 10 mg/kg, iv dose 1 mg/kg. ^c After oral and intravenous administration to fed male beagle dogs (*n* = 3) at 3 mg/kg and 0.3 mg/kg, respectively. *V*_{ss} volume of distribution; nd not determined.

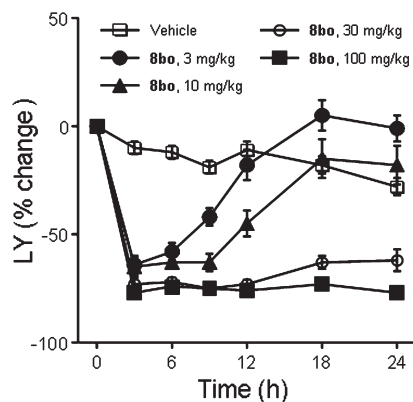
Evaluation of in Vivo Efficacy

The potency of compounds **8g** and **8bl** to **8bn** justified evaluating these compounds in vivo. Hence, the number of lymphocytes circulating in blood was measured just before, 3, 6, and 24 h after oral administration of the compound to male Wistar rats. Because of significant interindividual variability and the circadian rhythm of the number of circulating lymphocytes, a compound showing relative changes in the range of −20% to +40% is considered inactive. On the other hand, a lymphocyte count (LC) reduction in the range of −60 to −75% represents the maximal effect to be observed under the conditions of the experiment. Following these rules, compounds **8g** and **8bl** are clearly inactive at an oral dose of 10 (Table 7) and 30 mg/kg (data not shown). Subsequent pharmacokinetic (PK) experiments unravelled the reason for the lack of oral efficacy of these compounds (Table 8). The maximal plasma concentration (*C*_{max}) after oral administration of 3 mg/kg of **8bl** reached 8.1 ng/mL only. The clearance of the compound determined in a corresponding iv experiment was found to be close to total liver blood flow. These results demonstrate that **8bl** is not bioavailable. An almost identical PK profile was seen for the related compound **8t**. The high clearance of **8t** and **8bl** found in the PK experiment was also reflected in a high in vitro intrinsic clearance in rat hepatocytes. These results and the fact that phenols are well-known substrates for conjugating enzymes (see e.g., refs 91–93) made us speculate that the phenol function present in compound **8g** and **8bl** (and **8t**) is at least partially responsible for poor bioavailability and hence the lack of in vivo efficacy. Indeed, the compounds **8bf** and **8bm** (see Tables 5 and 6, respectively), wherein the phenol function was masked by a 2-hydroxy-ethyl group, showed significantly lower in vitro intrinsic and in vivo clearance values (Table 8). Both compounds gave reasonable concentrations in plasma (see e.g. *C*_{max}) and acceptable bioavailabilities. As a consequence, compound **8bm** showed a significant reduction in circulating lymphocytes 3 and 6 h after oral administration of 10 mg/kg (Table 7). Because of its almost 10 times lower potency on S1P₁, compound **8bf** (Table 5) had to be dosed at 100 mg/kg in order to evoke a comparable LC reduction (data not shown). As illustrated by example **8bn**, compounds incorporating a 2,3-dihydroxy-propoxy side chain at the benzylidene moiety showed favorable pharmacokinetic behavior too (Table 8). The racemate **8bn** maintained maximal LC reduction between 3 and 6 h after oral administration of 10 mg/kg. In fact, from the array of

Table 9. Potency of Compound **8bo** and S1P on All Five Human S1P Receptors as Determined in a GTP γ S, and 33 P–S1P Binding Assay^a

	GTP γ S EC ₅₀ [nM]					binding IC ₅₀ [nM]				
	S1P ₁	S1P ₂	S1P ₃	S1P ₄	S1P ₅	S1P ₁	S1P ₂	S1P ₃	S1P ₄	S1P ₅
8bo	5.7 ^b	> 10000	105	1108 ^c	59.1 ^d	6.0	> 10000	2068	1956	142
	1.2		1.3	1.2	1.9	1.4		1.2	1.5	1.2
	<i>n</i> = 5	<i>n</i> = 3	<i>n</i> = 5	<i>n</i> = 2	<i>n</i> = 4	<i>n</i> = 8	<i>n</i> = 4	<i>n</i> = 3	<i>n</i> = 4	<i>n</i> = 7
S1P	25.3	43.9	0.7	164	121	0.1	0.7	0.2	2.9	0.2
	1.1	1.2	1.3	1.2	1.2	1.1	1.1	1.1	1.1	1.1
	<i>n</i> = 5	<i>n</i> = 3	<i>n</i> = 5	<i>n</i> = 2	<i>n</i> = 4	<i>n</i> = 4	<i>n</i> = 4	<i>n</i> = 4	<i>n</i> = 4	<i>n</i> = 4

^a Values given as geometric means (first row), corresponding geometric standard deviation (second row), and number of independent experiments (third row). ^b The potency of **8bo** on the S1P₁ was slightly shifted to a lower value in this set of experiments, which is independent of the experiments performed to establish the SAR (Table 6). ^c Compound **8bo** acts as a partial agonist only, maximal activity of **8bo** at 10 μ M corresponds to 18% of the effect induced by S1P. ^d Maximal effect at 10 μ M reaches 42% of the effect of S1P.

**Figure 5.** Effect on lymphocyte counts in the blood 3, 6, 9, 12, 18, and 24 h after oral administration of vehicle (□), and 3 (●), 10 (▲), 30 (○) and 100 (■) mg/kg of **8bo** to male Wistar rats.

2-imino-thiazolidin-4-ones prepared for this study, this compound emerged as particularly interesting due to its high affinity for the S1P₁ receptor, its selectivity against S1P₃, and its in vivo efficacy. The individual enantiomers **8bo** and **8bp** are nearly equipotent in vitro (Table 6). However, the in vivo efficacy, in particular the duration of action of the (*R*)-enantiomer **8bo**, appears to be slightly better than the one of the (*S*)-enantiomer **8bp** (Table 7). It was therefore decided to study compound **8bo** in more detail. First, the selectivity profile of compound **8bo** with respect to all five S1P receptors was determined in a GTP γ S as well as a 33 P–S1P binding assay using membranes of recombinant chinese hamster ovary (CHO) or human embryonic kidney (HEK293) cells (for details see Experimental Section and Supporting Information). The results for compound **8bo** as well as those for the natural ligand S1P are compiled in Table 9. The binding assay confirms that the natural ligand S1P binds very tightly to all five S1P receptors. This is in clear contrast to the behavior of compound **8bo**, which shows a strong preference for the S1P₁ receptor not only in binding but also in the GTP γ S assay. Compound **8bo** binds less tightly to S1P₁ than S1P but at the same time appears to be the more potent agonist in the GTP γ S assay. In both the GTP γ S and the binding assay, **8bo** shows no affinity for the S1P₂ receptor. The absolute potency of **8bo** on S1P₃ differs significantly in the two assays. As a consequence the S1P₁ selectivity is about 20- and almost 350-fold in the GTP γ S and the binding assay, respectively. The affinities for the S1P₄ and S1P₅ receptor are in the μ M and 100 nM range, respectively. On S1P₄, **8bo** is not only less potent than S1P but also significantly less efficacious. Even at 10 μ M, **8bo** shows only 18% of the effect of S1P. A similar pattern is seen for the

S1P₅ receptor. Although **8bo** is a slightly more potent agonist than S1P, it never reaches the efficacy of the natural ligand. In conclusion, compound **8bo**, in particular when compared to S1P, is best described as a potent, selective, and fully efficacious S1P₁ receptor agonist.

In vivo dose response experiments in male Wistar rats clearly demonstrated that the maximal lymphocyte reduction of –65 to –75% is reached with a dose of 3 mg/kg (Figure 5). With increasing doses, the duration of action increased significantly. While a dose of 3 mg/kg showed maximal LC reduction for about 3 h, a dose of 100 mg/kg maintained a maximal effect for about 24 h. Nevertheless, even at this high dose, the LCs recovered completely within less than 36 h (data not shown), demonstrating the rapid reversibility of the lymphocyte sequestration. More details on lymphocyte subtype sequestration after multiple dosing in rats have been presented elsewhere.⁹⁴ The pharmacokinetic behavior of compound **8bo** was also studied in male beagle dogs (Table 8). These studies revealed a favorable bioavailability of 69%. The maximal plasma concentration of 1360 ng/mL was reached between 4 and 8 h after oral administration of 3 mg/kg. The half-life of compound **8bo** was found to be around 10 h. A single oral dose of 5 mg/kg caused maximal reduction of LC for at least 24 h in beagle dogs. Comparison of the in vitro intrinsic clearance in rat, dog, and human liver microsomes as well as hepatocytes (Table 8) indicates that the dog is more suitable to predict human PK properties. The in vivo efficacy data, together with the pharmacokinetic profile, in particular in the dog, suggested that **8bo** is suitable for a once daily dosing regimen in humans. This was confirmed in a single-ascending-dose human study wherein compound **8bo** showed good exposure and a half-life of 22–33 h.⁹⁵

Conclusion

In this account, we report on the discovery, preparation, and characterization of a novel class of 2-imino-thiazolidin-4-ones that serve as S1P₁ receptor agonists. The factors that influence the regioselectivity during the assembly of the 2-alkylimino-3-phenyl-thiazolidin-4-one scaffold are discussed. Detailed SAR studies led to the identification of the potent, selective, and orally active S1P₁ agonist **8bo**. In contrast to FTY720,^{32,34} **8bo** does not need to be phosphorylated in order to be active as an S1P₁ receptor agonist. Compound **8bo** showed maximal reduction of circulating lymphocytes at an oral dose of 3 mg/kg in Wistar rats. LCs were reduced for about 24 h when an oral dose of 100 mg/kg was administered. At this dose, lymphocyte sequestration was fully reversible within 36 h, reflecting the rapid decrease in the plasma concentration of **8bo**. This indicates quick recovery of

lymphocyte circulation upon discontinuation of **8bo**. In addition, **8bo** showed a favorable pharmacokinetic behavior in the dog. Meanwhile, compound **8bo** (ACT-128800) has undergone extensive toxicity testing and is now evaluated in clinical trials. First results of the entry-into-humans study demonstrate that the compound is suitable for once-a-day dosing.⁹⁵ More details shall be communicated in due course.

Experimental Section

Chemistry. All reagents and solvents were used as purchased from commercial sources (Sigma-Aldrich, Switzerland, Lancaster Synthesis GmbH, Germany, Acros Organics, USA). Moisture sensitive reactions were carried out under an argon atmosphere. Progress of the reactions was followed either by thin-layer chromatography (TLC) analysis (Merck, 0.2 mm silica gel 60 F₂₅₄ on glass plates) or by LC-MS. LC-MS: Finnigan MSQ plus or MSQ surveyor (Dionex, Switzerland) with HP 1100 binary pump and DAD (Agilent, Switzerland); column, Zorbax SB-AQ, 5 μ m, 120 Å, 4.6 mm \times 50 mm (Agilent); gradient, 5–95% acetonitrile in water containing 0.04% of trifluoroacetic acid, within 1 min; flow, 4.5 mL/min; t_R is given in min. Purity of the target compounds was confirmed on two additional columns: on a Zorbax Extend C18, 5 μ m, 80 Å, 4.6 mm \times 50 mm (Agilent), eluting with a gradient of 5–95% of acetonitrile in water containing 13 mM of NH₃; and on a Waters XBridge C18, OBD, 5 μ m, 4.6 mm \times 50 mm (Waters, Switzerland), eluting with a gradient of 5–95% of acetonitrile in water containing 13 mM of NH₃. According to these three LC-MS analyses, all compounds showed a purity >95% (UV at 230 nm), about half of the compounds showed a purity >98%. Purity and identity was further confirmed by NMR spectroscopy and, for some compounds, by combustion analysis (performed by Solvias AG, Basel, Switzerland). Prep HPLC: Waters XBridge Prep C18, 5 μ m, OBD, 19 mm \times 50 mm, gradient of acetonitrile in water containing 0.4% of formic acid, flow 75 mL/min. Melting points were determined by differential scanning calorimetry (DSC) using a DSC822e/400 instrument and the HSS7 sensor from Mettler Toledo, Switzerland. The sample was weighed in a 40 μ L aluminum crucible which was open (pierced pan) under a flow of 15 mL/min of nitrogen during the experiment. The scan goes from 20 to 320 °C at a rate of 5 K/min. The peak temperature of the melting endotherm was determined with the STARe software and was assigned to the melting point. pK_a values were determined with the GLpKa instrument from Sirius (United Kingdom) using pH-metric titrations with cosolvent; the cosolvent mixtures were water with 30, 40, and 50% (w/w) of methanol, and the ionic strength was adjusted with potassium chloride at a concentration of 0.15 M. The experimental temperature was 25 \pm 1 °C. The RefinementPro's built-in Yasuda–Shedlovski extrapolation technique at 0% methanol gave the pK_a . NMR spectroscopy: Bruker Avance II, 400 MHz UltraShield, ¹H (400 MHz), ¹³C (100 MHz), ¹⁹F (376 MHz) (Bruker, Switzerland); chemical shifts are reported in parts per million (ppm) relative to tetramethylsilane (TMS), and multiplicities are given as s (singlet), d (doublet), t (triplet), q (quartet), quint (quintuplet), h (hexet), hept (heptuplet), or m (multiplet). For compounds **3a**, **3b**, **3h**, **5a**, **5b**, **5i**, **5j**, **4a**, **4b**, **4h**, **6a**, **6b**, **6i**, and **6j**, structural assignment was corroborated by HMBC experiments, H–C correlations were established by HSQC experiments. In the ¹H and ¹³C NMR spectra of compounds bearing an ortho substituent at the 3-phenyl ring of the 2-alkylimino-3-phenyl-thiazolidin-4-one scaffolds, the signals of the 2-alkylimino substituent indicate the presence of atropisomers (e.g., compounds **3b**, **3q**, **5b**, **5f**, **8t**, **8y**, **8bn**, **8bo**, **8bp**). X-ray diffraction: To determine the molecular structure of compounds **2**, **5b**, **8e** and **8g**, a crystal of the corresponding compound was mounted on a Bruker Nonius diffractometer equipped with a CCD detector and reflections were measured using monochromatic Mo K α radi-

tion. The structure was solved by direct methods using SIR92, and refinement was performed with CRYSTALS. Full matrix least-squares refinement was performed with anisotropic temperature factors for all atoms except hydrogen, which were included at calculated positions with isotropic temperature factors. Coordinates, anisotropic temperature factors, bond lengths, and angles are deposited with the Cambridge Crystallographic Data Centre. In vitro potency assessment: Data (EC₅₀) are given as geometric means (\bar{X}_{geo}) with geometric standard deviation (σ_g). The upper and lower 95% confidence limits are calculated as $\bar{X}_{geo} \times \sigma_g^{-2}$ and $\bar{X}_{geo}/\sigma_g^{-2}$, respectively (results not shown). GTP γ S binding assays were performed in 96-well polypropylene microtiter plates in a final volume of 200 μ L. Membrane preparations of CHO cells expressing recombinant rat, dog, or human SIP₁, SIP₂, SIP₃, SIP₄, or SIP₅ receptors were used. Assay conditions were 20 mM Hepes, pH 7.4, 100 mM NaCl, 5 mM MgCl₂, 0.1% fatty acid free BSA, 1 or 3 μ M GDP (for SIP₁ or SIP₃, respectively), 2.5% DMSO, and 50 pM ³⁵S-GTP γ S. Test compounds were dissolved and diluted and preincubated with the membranes, in the absence of ³⁵S-GTP γ S, in 150 μ L assay buffer at room temperature for 30 min. After addition of 50 μ L of ³⁵S-GTP γ S in assay buffer, the reaction mixture was incubated for 1 h at room temperature. The assay was terminated by filtration of the reaction mixture through a Multiscreen GF/C plate (Filterplate from Millipore, MAHFC1H60), prewetted with ice-cold 50 mM Hepes pH 7.4, 100 mM NaCl, 5 mM MgCl₂, 0.4% fatty acid free BSA, using a Cell Harvester from Packard Biosciences. The filterplates were washed with ice-cold 10 mM Na₂HPO₄/NaH₂PO₄ (70%/30%) and dried. The plates were sealed, 25 μ L MicroScint20 was added, and membrane-bound ³⁵S-GTP γ S was determined on the Top-Count (Packard Biosciences). Specific ³⁵S-GTP γ S binding was determined by subtracting nonspecific binding (the signal obtained in the absence of agonist) from maximal binding (the signal obtained with 10 μ M SIP). The EC₅₀ of a test compound is the concentration of a compound inducing 50% of specific binding. Each compound was measured in three independent assays to obtain an average EC₅₀ from triplicate measurements.

The in vivo efficacy of the compounds **8** was assessed by measuring the circulating lymphocytes after oral administration of 3–100 mg/kg of a compound **8** to normotensive male Wistar rats. The animals were housed in climate-controlled conditions with a 12 h light/dark cycle and had free access to normal rat chow and drinking water. Blood was collected before and 3, 6, and 24 h after drug administration. Full blood was subjected to hematology using Beckman Coulter Ac-T 5diff CP (Beckman Coulter International SA, Nyon, Switzerland). All data are presented as mean \pm SEM. Statistical analyses were performed by analysis of variance (ANOVA) using Statistica (StatSoft) and the Student–Newman–Keuls procedure for multiple comparisons. The null hypothesis was rejected when $p < 0.05$. For formulation, the compounds were dissolved in DMSO. This solution was added to a stirred solution of gelatin (7.5%) in water. The resulting milky suspension containing a final concentration of 5% of DMSO was administered to the animals by gavage. A mixture of 95% of gelatin (7.5%) in water and 5% of DMSO served as vehicle.

(Z)-2-Isopropylimino-3-phenyl-thiazolidin-4-one (3a) (Method A). To a solution of isopropylamine (1.31 g, 1.91 mL, 22.2 mmol) in methanol (25 mL), phenyl isothiocyanate (3.00 g, 2.66 mL, 22.2 mmol) is added portionwise. The mixture which became slightly warm (approximately 30 °C) was stirred at room temperature for 3.5 h before bromoacetic acid methyl ester (3.39 g, 2.04 mL, 22.2 mmol) followed by pyridine (2.63 g, 2.68 mL, 33.3 mmol) was added. Stirring of the colorless reaction mixture was continued for 16 h. The resulting fine suspension was diluted with 1 N aq HCl (100 mL) and extracted with diethyl ether (150 mL). The separated organic phase contains crude **4a**. The pH of the aqueous phase was adjusted

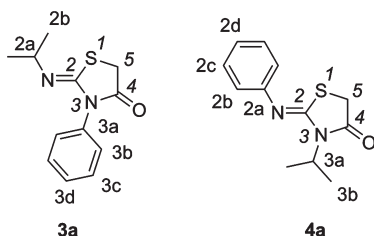


Figure 6. Atom numbering of compounds **3a** and **4a** as used in the HMBC assignment.

to pH 8 by adding satd aq NaHCO_3 solution. The aqueous phase was extracted with diethyl ether (4×150 mL). The combined organic extracts containing crude **3a** were dried over MgSO_4 , filtered, and concentrated. The remaining crystalline solid was washed with heptane and dried under high vacuum to give **3a** as an off-white crystalline solid (4.60 g, 88%), mp 149 °C. ^1H NMR (CDCl_3): δ 1.14 (d, $J = 6.3$ Hz, 6 H, H2b), 3.52 (hept, $J = 6.0$ Hz, 1 H, H2a), 3.98 (s, 2 H, H5), 7.27–7.32 (m, 2 H, H3b), 7.37–7.44 (m, 1 H, H3d), 7.45–7.52 (m, 2 H, H3c). ^{13}C NMR (CDCl_3): δ 23.35 (C2b), 32.58 (C5), 53.86 (C2a), 128.03 (C3b), 128.41 (C3d), 128.97 (C3c), 135.30 (C3a), 149.30 (C2), 171.39 (C4). HMBC (CDCl_3): H2a \rightarrow C2, C2b; H2b \rightarrow C2, C2a; H3b \rightarrow C3a, C3d; H3c \rightarrow C3a, C3d; H3d \rightarrow C3a, C3b; H5 \rightarrow C2, C4. LC-MS (ES^+): t_R 0.59 min. m/z : 235 ($M + H$). The organic extract containing crude (*Z*)-3-isopropyl-2-phenylimino-thiazolidin-4-one (**4a**) was concentrated and the crude byproduct was purified by column chromatography on silica gel eluting with heptane:ethyl acetate 3:1 to give pure **4a** as a pale-yellow oil (278 mg, 5%). ^1H NMR (CDCl_3): δ 1.55 (d, $J = 7.0$ Hz, 6 H, H3b), 3.75 (s, 2 H, H5), 4.90 (hept, $J = 6.8$ Hz, 1 H, H3a), 6.97 (d, $J = 7.5$ Hz, 2 H, H2b), 7.16 (t, $J = 7.5$ Hz, 1 H, H2d), 7.37 (t, $J = 7.5$ Hz, 2 H, H2c). ^{13}C NMR (CDCl_3): δ 18.72 (C3b), 32.50 (C5), 48.04 (C3a), 120.92 (C2c), 124.48 (C2d), 129.10 (C2b), 148.36 (C2a), 154.14 (C2), 171.92 (C4). HMBC (CDCl_3): H2b \rightarrow C2a, C2c, C2d; H2c \rightarrow C2a, C2b, C2d; H2d \rightarrow C2b, C2c; H3a \rightarrow C2, C3b, C4; H3b \rightarrow C3a; H5 \rightarrow C2, C4. LC-MS (ES^+): t_R 0.98 min. m/z : 235 ($M + H$) (Figure 6).

(Z)-2-Propylimino-3-phenylthiazolidin-4-one (5a) (Method B). To a solution of phenylisothiocyanate (2.00 g, 14.8 mmol) in dichloromethane (20 mL), *n*-propylamine (875 mg, 1.23 mL, 14.8 mmol) was added portionwise at 20 °C. The solution was stirred at 20 °C for 15 min. The solution was cooled to 0 °C before bromo-acetyl bromide (2.99 g, 1.29 mL, 14.8 mmol) was added carefully such that the temperature did not rise above 5 °C. The reaction mixture was stirred at 0 °C for 15 min before pyridine (2.40 g, 2.45 mL, 30.3 mmol) was added at 0 °C. The mixture was stirred for another 15 min at 0 °C, then warmed to 20 °C and washed with water (10 mL). The aqueous layer is extracted with dichloromethane (10 mL). The solvent of combined organic extracts was evaporated under reduced pressure to afford **5a** (1.84 g, 53%) as an off-white solid, mp 138 °C. This material was sufficiently pure (>90%) for further use in the substituted condensation step with substituted benzaldehydes. ^1H NMR (CDCl_3): δ 0.92 (t, $J = 7.3$ Hz, 2 H, H2c), 1.61 (h, $J = 7.0$ Hz, 2 H, H2b), 3.28 (t, $J = 7.0$ Hz, 2 H, H2a), 4.00 (s, 2 H, H5), 7.28–7.32 (m, 2 H, H3b), 7.37–7.45 (m, 1 H, H3d), 7.47–7.53 (m, 2 H, H3c). ^{13}C NMR (CDCl_3): δ 11.86 (C2c), 23.57 (C2b), 32.56 (C5), 54.29 (C2a), 127.98 (C3b), 128.63 (C3d), 129.17 (C3c), 135.17 (C3a), 151.67 (C2), 171.37 (C4). HMBC (CDCl_3): H2a \rightarrow C2, C2b, C2c; H2b \rightarrow C2a, C2c; H2c \rightarrow C2a, C2b; H3b \rightarrow C3a, C3d; H3c \rightarrow C3a, C3b; H3d \rightarrow C3a, C3b; H5 \rightarrow C2, C4. LC-MS (ES^+): t_R 0.60 min. m/z : 235 ($M + H$) (Figure 7).

(Z)-3-Propyl-2-phenylimino-thiazolidin-4-one (6a). Method A. From phenylisothiocyanate (34 mg, 0.25 mmol) and *n*-propylamine (15 mg, 0.25 mmol), colorless oil (50 mg, 85%) after purification on prep TLC plates with heptane:ethyl acetate 4:1. ^1H NMR (CDCl_3): δ 1.00 (t, $J = 7.5$ Hz, 3 H, H3c), 1.79 (h, $J = 7.5$ Hz, 2 H, H3b), 3.82 (s, 2 H, H5), 3.85 (t, $J = 7.5$ Hz, 2 H, H3a),

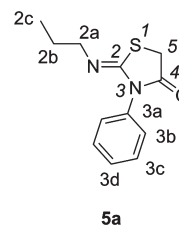


Figure 7. Atom numbering of compound **5a** as used in the HMBC assignment.

6.98 (d, $J = 7.3$ Hz, 2 H, H2b), 7.16 (t, $J = 7.5$ Hz, 1 H, H2d), 7.37 (t, $J = 7.8$ Hz, 2 H, H2c). ^{13}C NMR (CDCl_3): δ 11.29 (C3c), 20.56 (C3b), 32.72 (C5), 44.75 (C3a), 120.96 (C2c), 124.57 (C2d), 129.25 (C2b), 148.17 (C2a), 154.38 (C2), 171.83 (C4). HMBC (CDCl_3): H2b \rightarrow C2a, C2c, C2d; H2c \rightarrow C2a, C2b, C2d; H2d \rightarrow C2b, C2c; H3a \rightarrow C2, C3b, C3c, C4; H3b \rightarrow C3a, H3c; H3c \rightarrow C3a, C3b; H5 \rightarrow C2, C4. LC-MS (ES^+): t_R 0.96 min. m/z : 235 ($M + H$) (Figure 8).

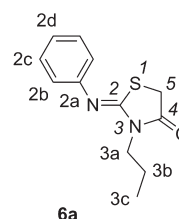


Figure 8. Atom numbering of compound **6a** as used in the HMBC assignment.

(Z)-2-Propylimino-3-phenylthiazolidin-4-one (5a) (Method C). A solution of aniline (20.4 g, 220 mmol) and triethylamine (33.3 g, 330 mmol) in THF (750 mL) was cooled to -70 °C before chloroacetyl chloride (24.8 g, 220 mmol) was added slowly over a period of about 30 min with vigorous stirring. The resulting suspension was warmed to room temperature, diluted with water (400 mL), and extracted with ethyl acetate (3×200 mL). The combined organic extracts were dried over MgSO_4 , filtered, and concentrated. The remaining fine platelets were washed with diethyl ether:heptane 1:1 and dried under high vacuum to give 2-chloro-*N*-phenyl-acetamide as fine pale-beige platelets (30.3 g, 82%), mp 136 °C. ^1H NMR (CDCl_3): δ 4.19 (s, 2 H), 7.19 (t, $J = 7.5$ Hz, 1 H), 7.37 (t, $J = 7.5$ Hz, 2 H), 7.56 (d, $J = 8.0$ Hz, 2 H), 8.34 (s br, 1 H). ^{13}C NMR (CDCl_3): δ 11.86, 23.57, 32.56, 54.29, 127.98, 128.63, 129.17, 135.17, 151.67, 171.37. LC-MS (ES^+): t_R 0.75 min. m/z : 170 ($M + H$). To a solution of 2-chloro-*N*-phenyl-acetamide (11.9 g, 70.0 mmol) and *n*-propyl isothiocyanate (7.07 g, 70.0 mmol) in DMF (200 mL), NaH (1.83 g, 55% dispersion in mineral oil, 42 mmol) was added in four portions every 20–30 min. Upon complete addition of NaH, stirring of the resulting brown mixture was continued for 2.5 h at rt. The mixture was diluted with ethyl acetate (500 mL) and extracted with 1 N aq HCl (2×200 mL). The combined aqueous extracts were extracted with ethyl acetate (2×200 mL) after their pH had been adjusted to pH 8 by adding satd aq NaHCO_3 -solution. These second organic extracts were washed with water (2×200 mL) and concentrated. The remaining solid was suspended in diethyl ether/hexane, filtered, washed with additional diethyl ether/hexane, and dried to give **5a** (4.85 g, 30%) as a pale-yellow powder, mp 143.6 °C. Spectroscopic data were identical to those of **5a** prepared according to method B.

(Z,Z)-2-(Dimethyl-hydrazono)-5-(4-hydroxy-3-methoxy-benzylidene)-3-phenylthiazolidin-4-one (2) (Method D). A solution of (*Z*)-2-(dimethyl-hydrazono)-3-phenylthiazolidin-4-one **9a** (118 mg, 0.50 mmol) and vanilline (84 mg, 0.55 mmol) in ethanol (2 mL) and piperidine (100 μL) was stirred at 80 °C for 18 h. The mixture was cooled to room temperature, diluted with diethyl ether (2 mL), and the precipitate that formed was collected,

washed with additional diethyl ether (2 × 10 mL), and dried under high vacuum to give the title compound (150 mg, 81%) as a yellow powder, mp 195 °C. ¹H NMR (CDCl₃): δ 2.57 (s, 6 H), 4.00 (s, 3 H), 7.04 (d, *J* = 8.3 Hz, 1 H), 7.08 (s, 1 H), 7.23 (d, *J* = 8.3 Hz, 1 H), 7.40–7.46 (m, 3 H), 7.49–7.56 (m, 2 H), 7.72 (s, 1 H). LC-MS (ES⁺): *t*_R 0.96 min. *m/z*: 370 (M + H). In another experiment following the above procedure, compound **2** cocrystallized with 1 equiv of piperidine. For analytical data and X-ray crystallographic structure parameters of the piperidinium salt of **2**, see the Supporting Information.

(Z,Z)-5-(3-Chloro-4-hydroxy-benzylidene)-2-(dimethyl-hydrazono)-3-phenyl-thiazolidin-4-one (8a) (Method E). A solution of (Z)-2-(dimethyl-hydrazono)-3-phenyl-thiazolidin-4-one **9a** (235 mg, 1.00 mmol), 3-chloro-4-hydroxy-benzaldehyde (235 mg, 1.00 mmol), and sodium acetate (164 mg, 2.00 mmol) in acetic acid (5 mL) is stirred at 85 °C for 18 h. The solution turned yellow and a precipitate formed. The mixture was cooled to rt, diluted with diethyl ether (150 mL), and washed with water (2 × 100 mL), satd aq NaHCO₃ solution (1 × 100 mL), and water (2 × 50 mL). The organic extract was dried over MgSO₄, filtered, and concentrated. The remaining residue was suspended and shortly refluxed in methanol (10 mL). The solid material was collected, washed with methanol, and dried under high vacuum to give the title compound as a bright-yellow powder (220 mg, 59%), mp >255 °C melting with decomposition. ¹H NMR (DMSO-*d*₆): δ 2.45 (s, 6 H), 7.16 (d, *J* = 8.5 Hz, 1 H), 7.40–7.48 (m, 3 H), 7.48–7.57 (m, 3 H), 7.63 (s, 1 H), 7.68 (s, 1 H), 11.02 (s br, 1 H). LC-MS (ES⁺): *t*_R 1.00 min. *m/z*: 374 (M + H). Anal. (C₁₈H₁₆ClN₃O₂SCl): C, H, N, O, S, Cl.

(Z,Z)-5-(3-Chloro-4-hydroxy-benzylidene)-2-isopropylimino-3-phenyl-thiazolidin-4-one (8g). Method E. The title compound (1.13 g, 71%) was isolated as a beige to yellow powder from the reaction mixture starting from **3a** (1.00 g, 4.27 mmol) and 3-chloro-4-hydroxy-benzaldehyde (668 mg, 4.27 mmol); mp 268 °C. ¹H NMR (DMSO-*d*₆): δ 1.11 (d, *J* = 6.0 Hz, 6 H), 3.56 (hept, *J* = 5.8 Hz, 1 H), 7.15 (d, *J* = 8.5 Hz, 1 H), 7.37 (d, *J* = 7.5 Hz, 2 H), 7.44 (d, *J* = 7.3 Hz, 1 H), 7.51 (t, *J* = 7.8 Hz, 3 H), 7.66 (s, 1 H), 7.69 (d, *J* = 1.0 Hz, 1 H), 10.99 (s, 1 H). LC-MS (ES⁺): *t*_R 1.01 min. *m/z*: 373 (M + H). Anal. (C₁₉H₁₇N₂O₂SCl): C, H, N, O, S, Cl. A small sample was recrystallized from ethanol/DCM to obtain crystals suitable for X-ray analysis, pale-yellow needles, mp 268 °C. X-ray crystallographic structure parameters: Crystals of **8g** (C₁₉H₁₇ClN₂O₂S, formula weight 372.87) formed in the triclinic space group *P*1̄. A total of 29341 reflections was measured at 173 K. Molecules/unit cell *Z* = 2, cell dimensions *a* = 9.2574(2) Å, *b* = 9.8000(2) Å, *c* = 10.6365(2) Å, α = 99.1910(10)°, β = 99.6080(10)°, γ = 108.6490(10)°; calculated density = 1.41 g cm⁻³. The final *R* factor of 0.031 was obtained for 4805 observed reflections (*I* > 3σ(*I*)); largest difference peak and hole were 0.42 and -0.41 eÅ⁻³, respectively (CCDC771349).

(Z,Z)-5-(3-Chloro-4-hydroxy-benzylidene)-2-propylimino-3-*o*-tolyl-thiazolidin-4-one (8bl). Method E. The title compound (1.14 mg, 69%) was isolated from the reaction mixture as a pale-yellow crystalline solid starting from **5b** (1.06 g, 4.27 mmol) and 3-chloro-4-hydroxy-benzaldehyde (668 mg, 4.27 mmol); mp 200 °C. ¹H NMR (DMSO-*d*₆): δ 0.84 (t, *J* = 7.3 Hz, 3 H), 1.46–1.57 (m, 2 H), 2.09 (s, 3 H), 3.24–3.37 (m, 2 H), 7.15 (d, *J* = 8.5 Hz, 1 H), 7.25–7.28 (m, 1 H), 7.30–7.36 (m, 1 H), 7.36–7.40 (m, 2 H), 7.53 (dd, *J* = 8.5, 2.0 Hz, 1 H), 7.67 (s, 1 H), 7.71 (d, *J* = 2.3 Hz, 1 H), 11.01 (s, 1 H). LC-MS (ES⁺): *t*_R 1.03 min. *m/z*: 387 (M + H). Anal. (C₂₀H₁₉N₂O₂SCl): C, H, N, S, Cl.

(Z,Z)-5-[3-Chloro-4-(2-hydroxy-ethoxy)-benzylidene]-2-propylimino-3-*o*-tolyl-thiazolidin-4-one (8bm). A mixture of 3-chloro-4-hydroxybenzaldehyde (10 g, 63.9 mmol), K₂CO₃ (26.5 g, 191.6 mmol), and 2-bromoethyl acetate (26.7 g, 159.7 mmol) in acetone (250 mL) was refluxed for 18 h before it was diluted with diethyl ether (200 mL) and washed with water (3 × 200 mL). The washings were extracted with diethyl ether (200 mL). The combined organic extracts were dried over MgSO₄ and concentrated. The remaining residue was purified by column chroma-

tography on silica gel eluting with heptane:ethyl acetate 1:1 to afford 3-chloro-4-(2-acetoxy-ethoxy)-benzaldehyde (6.44 g, 42%) as colorless solid. ¹H NMR (CDCl₃): δ 2.12 (s, 3H), 4.35–4.31 (m, 2H), 4.53–4.49 (m, 2H), 7.03 (d, *J* = 8.8 Hz, 1H), 7.75 (dd, *J* = 1.8, 8.2 Hz, 1H), 7.91 (d, *J* = 1.8 Hz, 1H), 9.85 (s, 1H). LC: *t*_R 0.88 min. The title compound (276 mg, 80%) was obtained as a pale-yellow foam after purification on prep. TLC plates with heptane:EA 1:1 in analogy to compound **8bc** starting from **5b** (200 mg, 0.81 mmol) and the above 3-chloro-4-(2-acetoxy-ethoxy)-benzaldehyde (391 mg, 1.61 mmol). ¹H NMR (CDCl₃): δ 0.94 (t, *J* = 7.5 Hz, 3 H), 1.60–1.70 (m, 2 H), 2.22 (s, 3 H), 3.34–3.48 (m, 2 H), 4.05 (t br, *J* = 4.3 Hz, 2 H), 4.24 (t, *J* = 4.3 Hz, 2 H), 7.07 (d, *J* = 8.5 Hz, 1 H), 7.21 (d, *J* = 7.3 Hz, 1 H), 7.32–7.39 (m, 3 H), 7.48 (dd, *J* = 8.5, 2.3 Hz, 1 H), 7.65 (d, *J* = 2.3 Hz, 1 H), 7.69 (s, 1 H). LC-MS (ES⁺): *t*_R 1.04 min. *m/z*: 431 (M + H). Anal. (C₂₂H₂₃N₂O₃SCl): C, H, N, O, S, Cl, ash <0.2%.

***rac*-(Z,Z)-5-[3-Chloro-4-(2,3-dihydroxy-propoxy)-benzylidene]-2-propylimino-3-*o*-tolyl-thiazolidin-4-one (8bn)**. Method E. Starting from **5b** (450 mg, 1.81 mmol) and *rac*-4-(2,3-dihydroxy-propoxy)-3-chloro-benzaldehyde (835 mg, 3.62 mmol), the title compound (262 mg, 32%) was obtained as a white powder after extractive workup and purification of the crude product on prep. TLC plates with toluene:ethyl acetate 1:3. ¹H NMR (CDCl₃): δ 0.94 (t, *J* = 7.3 Hz, 3 H), 1.60–1.70 (m, 2 H), 2.12 (t br, *J* = 5.8 Hz, 1 H), 2.21 (s, 3 H), 2.76 (d br, *J* = 3.8 Hz, 1 H), 3.34–3.48 (m, 2 H), 3.83–3.97 (m, 2 H), 4.17–4.27 (m, 3 H), 7.07 (d, *J* = 8.5 Hz, 1 H), 7.21 (d, *J* = 7.3 Hz, 1 H), 7.31–7.39 (m, 3 H), 7.49 (dd, *J* = 8.8, 1.8 Hz, 1 H), 7.64 (d, *J* = 1.8 Hz, 1 H), 7.69 (s, 1 H). LC-MS (ES⁺): *t*_R 0.96 min. *m/z*: 461 (M + H). Anal. (C₂₃H₂₅N₂O₄SCl) H, N, S, Cl; C: calcd 59.93, found 60.41.

(Z,Z)-5-[3-Chloro-4-((2*R*)-2,3-dihydroxy-propoxy)-benzylidene]-2-propylimino-3-*o*-tolyl-thiazolidin-4-one (8bo). To a solution of 3-chloro-4-hydroxybenzaldehyde (4.21 g, 26.9 mmol) in degassed toluene (100 mL), ((4*S*)-2,2-dimethyl-[1,3]dioxolan-4-yl)-methanol (5.35 g, 40.5 mmol) and 1,1'-(azodicarbonyl)dipiperidine (13.63 g, 54 mmol) followed by tributylphosphine (10.93 g, 54 mmol) was added. The mixture became slightly warm and a precipitate formed. The reaction mixture was diluted with degassed toluene (500 mL) and was stirred at room temperature for 2 h, then at 60 °C for further 18 h before it was washed with 1 N aq NaOH (3 × 150 mL) and water (150 mL). The organic phase was collected, dried over MgSO₄, filtered, and concentrated to leave a dark-brown oil which was purified by column chromatography on silica gel eluting with hexane:ethyl acetate 4:1 to give 3-chloro-4-((4*S*)-2,2-dimethyl-[1,3]dioxolan-4-yl)-methoxy-benzaldehyde (4.30 g, 59%) as a yellow oil. LC: *t*_R 0.93 min. ¹H NMR (CDCl₃): δ 1.41 (s, 3H), 1.47 (s, 3H), 4.06–4.00 (m, 1H), 4.14–4.08 (m, 1H), 4.23–4.17 (m, 2H), 4.56–4.43 (m, 1H), 7.05 (d, *J* = 8.2 Hz, 1H), 7.74 (dd, *J* = 1.8, 8.2 Hz, 1H), 7.89 (d, *J* = 1.8 Hz, 1H), 9.82 (s, 1H). A solution of **5b** (1.98 g, 8.00 mmol), the above 3-chloro-4-((4*S*)-2,2-dimethyl-[1,3]dioxolan-4-yl)-methoxy-benzaldehyde (4.32 g, 16.0 mmol) and anhydrous sodium acetate (1.31 g, 16.0 mmol) in acetic acid (50 mL) was stirred at 110 °C for 4 h. Water (0.3 mL) was added, and stirring was continued at 100 °C for 1 h before the mixture was concentrated. The remaining residue was dissolved in ethyl acetate (250 mL), washed with satd aq NaHCO₃ solution (250 mL) and water (2 × 150 mL), dried over MgSO₄, filtered, and again concentrated. Sodium methoxide (500 mg, 9.25 mmol) was added to a solution of the residue in methanol (100 mL). The mixture was stirred at 40 °C for 30 min before it was concentrated. The remaining residue was dissolved in ethyl acetate (250 mL) and washed twice with water (2 × 150 mL). The washings were extracted back with ethyl acetate (150 mL), and the combined organic extracts were dried over MgSO₄, filtered, and concentrated. The crude product was purified by column chromatography on silica gel eluting with heptane:ethyl acetate 1:4 to give the title compound (1.34 g, 37%) as a pale-yellow foam. ¹H NMR (CDCl₃): δ 0.94 (t, *J* = 7.3 Hz, 3 H), 1.58–1.70 (m, 2 H), 2.21 (s, 3 H), 3.32–3.48 (m, 2 H), 3.82–3.95 (m, 3 H),

4.12–4.27 (m, 4 H), 7.07 (d, J = 8.8 Hz, 1 H), 7.21 (d, J = 7.0 Hz, 1 H), 7.31–7.39 (m, 3 H), 7.49 (dd, J = 8.5, 2.0 Hz, 1 H), 7.64 (d, J = 2.0 Hz, 1 H), 7.69 (s, 1 H). ^{13}C NMR (CDCl_3): δ 11.83, 17.68, 23.74, 55.42, 63.46, 69.85, 70.78, 133.48, 120.75, 123.71, 127.05, 128.25, 128.60, 129.43, 130.06, 131.13, 131.50, 134.42, 136.19, 146.98, 154.75, 166.12. LC-MS (ES^+): t_{R} 0.96 min. m/z : 461 ($\text{M} + \text{H}$). HPLC (ChiralPak AD-H, 4.6 mm \times 250 mm, 0.8 mL/min, 70% hexane in ethanol): t_{R} 11.8 min. Anal. ($\text{C}_{23}\text{H}_{25}\text{N}_2\text{O}_4\text{SCl}$): C, H, N, O, S, Cl.

(**Z**)-5-[3-Chloro-4-((2*S*)-2,3-dihydroxy-propoxy)-benzylidene]-2-propylimino-3-*o*-tolyl-thiazolidin-4-one (**8bp**). Starting from 3-chloro-4-hydroxybenzaldehyde (2.00 g, 12.8 mmol) and ((4*R*)-2,2-dimethyl-[1,3]dioxolan-4-yl)-methanol (2.53 g, 19.2 mmol), 3-chloro-4-((4*R*)-2,2-dimethyl-[1,3]dioxolan-4-ylmethoxy)-benzaldehyde (1.95 g, 56%) was obtained as a brownish oil following the procedure given above for its (*S*)-isomer. LC: t_{R} 0.93 min. ^1H NMR (CDCl_3): δ 1.43 (s, 3 H), 1.49 (s, 3 H), 4.06 (dd, J = 8.5, 5.8 Hz, 1 H), 4.11–4.18 (m, 1 H), 4.20–4.26 (m, 2 H), 4.52–4.59 (m, 1 H), 7.09 (d, J = 8.5 Hz, 1 H), 7.78 (dd, J = 8.5, 2.0 Hz, 1 H), 7.93 (d, J = 2.0 Hz, 1 H), 9.88 (s, 1 H). Starting from **5b** (248 mg, 1.00 mmol) and the above 3-chloro-4-((4*R*)-2,2-dimethyl-[1,3]dioxolan-4-ylmethoxy)-benzaldehyde (405 mg, 1.50 mmol), the title compound (210 mg, 46%) was obtained as a pale-yellow solid following the procedure given for compound **8bo**. ^1H NMR (CDCl_3): δ 0.94 (t, J = 7.4 Hz, 3 H), 1.59–1.72 (m, 2 H), 2.21 (s, 3 H), 2.31 (s br, 1 H), 2.90 (s br, 1 H), 3.34–3.48 (m, 2 H), 3.80–3.95 (m, 2 H), 4.15–4.25 (m, 3 H), 7.06 (d, J = 8.6 Hz, 1 H), 7.21 (d, J = 7.2 Hz, 1 H), 7.31–7.40 (m, 3 H), 7.48 (dd, J = 8.6, 2.1 Hz, 1 H), 7.63 (d, J = 2.1 Hz, 1 H), 7.67 (s, 1 H). LC-MS (ES^+): t_{R} 0.96 min, m/z : 461 ($\text{M} + \text{H}$). HPLC (ChiralPak AD-H, 4.6 mm \times 250 mm, 0.8 mL/min, 70% hexane in ethanol): t_{R} 13.6 min. Anal. ($\text{C}_{23}\text{H}_{25}\text{N}_2\text{O}_4\text{SCl}$, 0.1 H_2O): C, H, N, O, S, Cl, ash < 0.2%.

Acknowledgment. We gratefully acknowledge the excellent work done by our co-workers Céline Bortolamiol, Stéphane Delahaye, Judith Frei, Hakim Hadana, Julie Hoerner, Katalin Menyhart, Christine Metzger, Rodolphe Mielke, David Monnard, Markus Rey, Christine Seeger, Jürgen Seifert, Marco Tschanz, Gaby von Aesch, Daniel Wanner, and Aude Weigel, and Martine Clozel and Walter Fischli for support.

Note Added in Proof. Reference 51 has been retracted by Premenko-Lanier et al., *Nature* **2010**, 464, 942 (8 April 2010).

Supporting Information Available: Experimental details on the synthesis and characterization, including biological assays, of the 2-imino-thiazolidin-4-one scaffolds **3**, **4**, **5**, **6**, additional 2-imino-thiazolidin-4-one scaffolds, and target compounds **8** prepared for this study. This material is available free of charge via the Internet at <http://pubs.acs.org>.

References

- Chun, J.; Goetzl, E. J.; Hla, T.; Igarashi, Y.; Lynch, K. R.; Moolenaar, W.; Pyne, S.; Tigyi, G. International Union of Pharmacology. XXXIV. Lysophospholipid Receptor Nomenclature. *Pharmacol. Rev.* **2002**, 54, 265–269.
- Ishii, I.; Fukushima, N.; Ye, X.; Chun, J. Lysophospholipid Receptors: Signaling and Biology. *Annu. Rev. Biochem.* **2004**, 73, 321–354.
- Brinkmann, V. Sphingosine 1-phosphate receptors in health and disease: Mechanistic insights from gene deletion studies and reverse pharmacology. *Pharmacol. Ther.* **2007**, 115, 84–105.
- Meyer-zu-Herford, D.; Jakobs, K. H. Lysophospholipid receptors: Signalling, pharmacology and regulation by lysophospholipid metabolism. *Biochim. Biophys. Acta* **2006**, 1768, 923–940.
- Gardell, S. E.; Dubi, A. E.; Chun, J. Emerging medicinal roles for lysophospholipid signaling. *Trends Mol. Med.* **2006**, 12, 65–75.
- Rosen, H.; Gonzalez-Cabrera, P. J.; Sanna, M. G.; Brown, S. Sphingosine 1-Phosphate Receptor Signaling. *Annu. Rev. Biochem.* **2009**, 78, 743–768.
- Maceyka, M.; Payne, S. G.; Milstien, S.; Spiegel, S. Sphingosine kinase, sphingosine-1-phosphate, and apoptosis. *Biochim. Biophys. Acta* **2002**, 1585, 193–201.
- Spiegel, S.; Milstien, S. Sphingosine-1-phosphate: An Enigmatic Signalling Lipid. *Nature Rev. Mol. Cell Biol.* **2003**, 4, 397–407.
- Hait, N. C.; Oskeritzian, C. A.; Paugh, S. W.; Milstien, S.; Spiegel, S. Sphingosine kinases, sphingosine 1-phosphate, apoptosis and diseases. *Biochim. Biophys. Acta* **2006**, 1758, 2016–2026.
- Kihara, A.; Mitsutake, S.; Mizutani, Y.; Igarashi, Y. Metabolism and biological functions of two phosphorylated sphingolipids, sphingosine 1-phosphate and ceramide 1-phosphate. *Prog. Lipid Res.* **2007**, 46, 126–144.
- Augé, N.; Nègre-Salvayre, A.; Salvayre, R.; Levade, T. Sphingomyelin metabolites in vascular cell signaling and atherogenesis. *Prog. Lipid Res.* **2000**, 39, 207–229.
- Alewijsse, A. E.; Peters, S. L. M.; Michel, M. C. Cardiovascular effects of sphingosine-1-phosphate and other sphingomyelin metabolites. *Br. J. Pharmacol.* **2004**, 143, 666–684.
- McVerry, B. J.; Garcia, J. G. N. In vitro and in vivo modulation of vascular barrier integrity by sphingosine 1-phosphate: mechanistic insights. *Cell. Signalling* **2005**, 17, 131–139.
- Yatomi, Y. Sphingosine 1-Phosphate in Vascular Biology: Possible Therapeutic Strategies to Control Vascular Disease. *Curr. Pharm. Des.* **2006**, 12, 575–587.
- Rosen, H.; Sanna, M. G.; Cahalan, S. M.; Gonzalez-Cabrera, P. J. Tipping the gatekeeper: S1P regulation of endothelial barrier function. *Trends Immunol.* **2007**, 28, 102–107.
- Michel, M. C.; Mulders, A. C. M.; Jongsma, M.; Alewijsse, A. E.; Peters, S. L. M. Vascular effects of sphingolipids. *Acta Paed.* **2007**, 96, 44–48.
- Alewijsse, A. E.; Peters, S. L. M. Sphingolipid signalling in the cardiovascular system: good, bad or both? *Eur. J. Pharmacol.* **2008**, 585, 292–302.
- Brinkmann, V.; Baumruker, T. Pulmonary and vascular pharmacology of sphingosine 1-phosphate. *Curr. Opin. Pharmacol.* **2006**, 6, 244–250.
- Uhlir, S.; Gulbins, E. Sphingolipids in the lungs. *Am. J. Resp. Crit. Care Med.* **2008**, 178, 1100–1114.
- Oskeritzian, C. A.; Milstien, S.; Spiegel, S. Sphingosine-1-phosphate in allergic responses, asthma and anaphylaxis. *Pharmacol. Ther.* **2007**, 115, 390–399.
- Rosen, H.; Goetzl, E. J. Sphingosine 1-phosphate and its receptors: an autocrine and paracrine network. *Nature Rev. Immunol.* **2005**, 5, 560–570.
- Rivera, J.; Proia, R. L.; Olivera, A. The alliance of sphingosine-1-phosphate and its receptors in immunity. *Nature Rev. Immunol.* **2008**, 8, 753–763.
- Okada, T.; Kajimoto, T.; Jahangeer, S.; Nakamura, S. Sphingosine kinase/sphingosine 1-phosphate signalling in central nervous system. *Cell. Signalling* **2009**, 21, 7–13.
- Milstien, S.; Gude, D.; Spiegel, S. Sphingosine 1-phosphate in neural signalling and function. *Acta Paed.* **2007**, 96, 40–43.
- Ishii, M.; Egen, J. G.; Klauschen, F.; Meier-Schellersheim, M.; Saeki, Y.; Vacher, J.; Proia, R. L.; Germain, R. N. Sphingosine-1-phosphate mobilizes osteoclast precursors and regulates bone homeostasis. *Nature* **2009**, 458, 524–528.
- Liu, F.; Verin, A. D.; Wang, P.; Day, R.; Wersto, R. P.; Chrest, F. J.; English, D. K.; Garcia, J. G. N. Differential Regulation of Sphingosine-1-Phosphate- and VEGF-Induced Endothelial Cell Chemotaxis. *Am. J. Respir. Cell Mol. Biol.* **2001**, 24, 711–719.
- Graeler, M.; Goetzl, E. J. Activation-regulated expression and chemotactic function of sphingosine 1-phosphate receptors in mouse splenic T cells. *FASEB J.* **2002**, 16, 1874–1878.
- Adachi, K.; Kohara, T.; Nakao, N.; Arita, M.; Chiba, K.; Mishina, T.; Sasaki, S.; Fujita, T. Design, synthesis, and structure–activity relationships of 2-substituted-2-amino-1,3-propanediols: discovery of a novel immunosuppressant, FTY720. *Bioorg. Med. Chem. Lett.* **1995**, 5, 853–856.
- Chiba, K.; Yanagawa, Y.; Masubuchi, Y.; Kataoka, H.; Kawaguchi, T.; Ohtsuki, M.; Hoshino, Y. FTY720, a Novel Immunosuppressant, Induces Sequestration of Circulating Mature Lymphocytes by Acceleration of Lymphocyte Homing in Rats. I. FTY720 Selectively Decreases the Number of Circulating Mature Lymphocytes by Acceleration of Lymphocyte Homing. *J. Immunol.* **1998**, 160, 5037–5044.
- Pinschewer, D. D.; Ochsenbein, A. F.; Odermatt, B.; Brinkmann, V.; Hengartner, H.; Zinkernagel, R. M. FTY720 Immunosuppression Impairs Effector T Cell Peripheral Homing Without Affecting Induction, Expansion, and Memory. *J. Immunol.* **2000**, 164, 5761–5770.

- (31) Brinkmann, V.; Chen, S.; Feng, L.; Pinschewer, D.; Nikolova, Z.; Hof, R. FTY720 Alters Lymphocyte Homing and Protects Allografts Without Inducing General Immunosuppression. *Transplant. Proc.* **2001**, *33*, 530–531.
- (32) Brinkmann, V.; Davis, M. D.; Heise, C. E.; Albert, R.; Cottens, S.; Hof, R.; Bruns, C.; Prieschl, E.; Baumruker, T.; Hiestand, P.; Foster, C. A.; Zollinger, M.; Lynch, K. R. The Immune Modulator FTY720 Targets Sphingosine 1-Phosphate Receptors. *J. Biol. Chem.* **2002**, *277*, 21453–21457.
- (33) Billich, A.; Bornancin, F.; Dévay, P.; Mechtcheriakova, D.; Urtz, N.; Baumruker, T. Phosphorylation of the Immunomodulatory Drug FTY720 by Sphingosine Kinases. *J. Biol. Chem.* **2003**, *278*, 47408–47415.
- (34) Mandala, S.; Hajdu, R.; Bergstrom, J.; Quackenbush, E.; Xie, J.; Milligan, J.; Thornton, R.; Shei, G.-J.; Card, D.; Keohane, C. A.; Rosenbach, M.; Hale, J.; Lynch, C. L.; Rupprecht, K.; Parsons, W.; Rosen, H. Alteration of Lymphocyte Trafficking by Sphingosine-1-Phosphate Receptor Agonists. *Science* **2002**, *296*, 346–349.
- (35) Albert, R.; Hinterding, K.; Brinkmann, V.; Guerini, D.; Müller-Hartwig, C.; Knecht, H.; Simeon, C.; Streiff, M.; Wagner, T.; Welzenbach, K.; Zéciri, F.; Zollinger, M.; Cooke, N.; Francotte, E. Novel Immunomodulator FTY720 Is Phosphorylated in Rats and Humans To Form a Single Stereoisomer. Identification, Chemical Proof, and Biological Characterization of the Biologically Active Species and Its Enantiomer. *J. Med. Chem.* **2005**, *48*, 5373–5377.
- (36) Allende, M. L.; Dreier, J. L.; Mandala, S.; Proia, R. L. Expression of the Sphingosine 1-Phosphate Receptor, SIP₁, on T-cells Controls Thymic Emigration. *J. Biol. Chem.* **2004**, *279*, 15396–15401.
- (37) Matloubian, M.; Lo, C. G.; Cinamon, G.; Lesneski, M. J.; Xu, Y.; Brinkmann, V.; Allende, M. L.; Proia, R. L.; Cyster, J. G. Lymphocyte egress from thymus and peripheral lymphoid organs is dependent on SIP receptor 1. *Nature* **2004**, *427*, 355–360.
- (38) Hale, J. J.; Neway, W.; Mills, S. G.; Hajdu, R.; Keohane, C. A.; Rosenbach, M.; Milligan, J.; Shei, G.-J.; Chrebet, G.; Bergstrom, J.; Card, D.; Koo, G. C.; Koprak, S. L.; Jackson, J. J.; Rosen, H.; Mandala, S. Potent SIP receptor agonists replicate the pharmacologic actions of the novel immune modulator FTY720. *Bioorg. Med. Chem. Lett.* **2004**, *14*, 3351–3355.
- (39) Jo, E.; Sanna, M. G.; Gonzalez-Cabrera, P. J.; Thangada, S.; Tigvi, G.; Osborne, D. A.; Hla, T.; Parrill, A. L.; Rosen, H. SIP₁-Selective In Vivo-Active Agonists from High-Throughput Screening: Off-the-Shelf Chemical Probes of Receptor Interactions, Signaling, and Fate. *Chem. Biol.* **2005**, *12*, 703–715.
- (40) Wei, S. H.; Rosen, H.; Matheu, M. P.; Sanna, M. G.; Wang, S.-K.; Jo, E.; Wong, C.-H.; Parker, I.; Cahalan, M. D. Sphingosine 1-phosphate type 1 receptor agonism inhibits transendothelial migration of medullary T cells to lymphatic sinuses. *Nature Immunol.* **2005**, *6*, 1228–1235.
- (41) Rosen, H.; Alfonso, C.; Surh, C. D.; McHeyzer-Williams, M. G. Rapid induction of medullary thymocyte phenotypic maturation and egress inhibition by nanomolar sphingosine 1-phosphate receptor agonist. *Proc. Natl. Acad. Sci. U.S.A.* **2003**, *100*, 10907–10912.
- (42) Hla, T.; Venkataraman, K.; Michaud, J. The vascular SIP gradient—cellular sources and biological significance. *Biochim. Biophys. Acta* **2008**, *1781*, 477–482.
- (43) Sinha, R. K.; Park, C.; Hwang, I.-Y.; Davis, M. D.; Kehrl, J. H. B Lymphocytes Exit Lymph Nodes through Cortical Lymphatic Sinusoids by a Mechanism Independent of Sphingosine-1-Phosphate-Mediated Chemotaxis. *Immunity* **2009**, *30*, 434–446.
- (44) Dorsam, G.; Graeler, M. H.; Seroogy, C.; Kong, Y.; Voice, J. K.; Goetzl, E. J. Transduction of Multiple Effects of Sphingosine 1-Phosphate (SIP) on T Cell Functions by the SIP₁ G Protein-Coupled Receptor. *J. Immunol.* **2003**, *171*, 3500–3507.
- (45) Schwab, S. R.; Cyster, J. G. Finding a way out: lymphocyte egress from lymphoid organs. *Nature Immunol.* **2007**, *8*, 1295–1301.
- (46) Pappu, R.; Schwab, S. R.; Cornelissen, I.; Pereira, J. P.; Regard, J. B.; Xu, Y.; Camerer, E.; Zheng, Y.-W.; Huang, Y.; Cyster, J. G.; Coughlin, S. R. Promotion of Lymphocyte Egress into Blood and Lymph by Distinct Sources of Sphingosine-1-Phosphate. *Science* **2007**, *316*, 295–298.
- (47) Sanna, M. G.; Wang, S.-K.; Gonzalez-Cabrera, P. J.; Don, A.; Marsolais, D.; Matheu, M. P.; Wei, S. H.; Parker, I.; Jo, E.; Cheng, W.-C.; Cahalan, M. D.; Wong, C.-H.; Rosen, H. Enhancement of capillary leakage and restoration of lymphocyte egress by a chiral SIP₁ antagonist in vivo. *Nature Chem. Biol.* **2006**, *8*, 434–441.
- (48) Marsolais, D.; Rosen, H. Chemical modulators of sphingosine-1-phosphate receptors as barrier-oriented therapeutic molecules. *Nature Rev. Drug Discovery* **2009**, *8*, 297–307.
- (49) Brinkmann, V.; Pinschewer, D. D.; Feng, L.; Chen, S. FTY720: Altered lymphocyte traffic results in allograft protection. *Transplantation* **2001**, *72*, 764–769.
- (50) Graeler, M. H.; Huang, M.-C.; Watson, S.; Goetzl, E. J. Immunological Effects of Transgenic Constitutive Expression of the Type 1 Sphingosine 1-Phosphate Receptor by Mouse Lymphocytes. *J. Immunol.* **2005**, *174*, 1997–2003.
- (51) Premenko-Lanier, M.; Moseley, N. B.; Pruett, S. T.; Romagnoli, P. A.; Altman, J. D. Transient FTY720 treatment promotes immune-mediated clearance of a chronic viral infection. *Nature* **2008**, *454*, 894–898.
- (52) Baumruker, T.; Billich, A.; Brinkmann, V. FTY720, an immunomodulatory sphingolipid mimetic: translation of a novel mechanism into clinical benefit in multiple sclerosis. *Expert Opin. Invest. Drugs* **2007**, *16*, 283–289.
- (53) Mansoor, M.; Melendez, A. J. Recent Trials for FTY720 (Fingolimod): A New Generation of Immunomodulators Structurally Similar to Sphingosine. *Rev. Recent Clin. Trials* **2008**, *3*, 62–69.
- (54) O'Connor, P.; Comi, G.; Montalban, X.; Antel, J.; Radue, E. W.; deVera, A.; Pohlmann, H.; Kappos, L. Oral fingolimod (FTY720) in multiple sclerosis. *Neurology* **2009**, *72*, 73–79.
- (55) Foster, C. A.; Howard, L. M.; Schweitzer, A.; Persohn, E.; Hiestand, P. C.; Balatoni, B.; Reuschel, R.; Beerli, C.; Schwartz, M.; Billich, A. Brain Penetration of the Oral Immunomodulatory Drug FTY720 and Its Phosphorylation in the Central Nervous System during Experimental Autoimmune Encephalomyelitis: Consequences for Mode of Action in Multiple Sclerosis. *J. Pharmacol. Exp. Ther.* **2007**, *323*, 469–476.
- (56) Balatoni, B.; Storch, M. K.; Swoboda, E.-M.; Schönborn, V.; Koziel, A.; Lambrou, G. N.; Hiestand, P. C.; Weissert, R.; Foster, C. A. FTY720 sustains and restores neuronal function in the DA rat model of MOG-induced experimental autoimmune encephalomyelitis. *Brain Res. Bull.* **2007**, *74*, 307–316.
- (57) Miron, V. E.; Hall, J. A.; Kennedy, T. E.; Soliven, B.; Antel, J. P. Cyclical and Dose-Dependent Responses of Adult Human Mature Oligodendrocytes to Fingolimod. *Am. J. Pathol.* **2008**, *173*, 1143–1152.
- (58) Miron, V. E.; Schubart, A.; Antel, J. P. Central nervous system-directed effects of FTY720 (fingolimod). *J. Neurol. Sci.* **2008**, *274*, 13–17.
- (59) Dev, K. K.; Mullershausen, F.; Mattes, H.; Kuhn, R. R.; Bilbe, G.; Hoyer, D.; Mir, A. Brain sphingosine-1-phosphate receptors: implication for FTY720 in the treatment of multiple sclerosis. *Pharmacol. Ther.* **2008**, *117*, 77–93.
- (60) Choi, J. W.; Herr, D.; Lee, C.-W.; Teo, S.; Kennedy, G.; Chun, J. SIP₁ receptor signaling on cells of astrocytic lineages in experimental autoimmune encephalomyelitis: a role in disease progression and the efficacy of fingolimod (FTY720). *Mult. Scler.* **2008**, *14* (S37), P29.
- (61) Hale, J. J.; Doherty, G.; Toth, L.; Mills, S. G.; Hajdu, R.; Keohane, C. A.; Rosenbach, M.; Milligan, J.; Shei, G.-J.; Chrebet, G.; Bergstrom, J.; Card, D.; Forrest, M.; Sun, S.-Y.; West, S.; Xie, H.; Nomura, N.; Rosen, H.; Mandala, S. Selecting against SIP₃ enhances the acute cardiovascular tolerability of 3-(N-benzyl)aminopropylphosphonic acid SIP receptor agonists. *Bioorg. Med. Chem. Lett.* **2004**, *14*, 3501–3505.
- (62) Forrest, M.; Sun, S.-Y.; Hajdu, R.; Bergstrom, J.; Card, D.; Doherty, G.; Hale, J.; Keohane, C.; Meyers, C.; Milligan, J.; Mills, S.; Nomura, N.; Rosen, H.; Rosenbach, M.; Shei, G.-J.; Singer, I. I.; Tian, M.; West, S.; White, V.; Xie, J.; Proia, R. L.; Mandala, S. Immune Cell Regulation and Cardiovascular Effects of Sphingosine 1-Phosphate Receptor Agonists in Rodents Are Mediated via Distinct Receptor Subtypes. *J. Pharmacol. Exp. Ther.* **2004**, *309*, 758–768.
- (63) Sanna, M. G.; Liao, J.; Jo, E.; Alfonso, C.; Ahn, M.-Y.; Peterson, M. S.; Webb, B.; Lefebvre, S.; Chun, J.; Gray, N.; Rosen, H. Sphingosine 1-Phosphate (SIP) Receptor Subtypes SIP₁ and SIP₃, Respectively, Regulate Lymphocyte Recirculation and Heart Rate. *J. Biol. Chem.* **2004**, *279*, 13839–13848.
- (64) Salomone, S.; Potts, E. M.; Tyndall, S.; Ip, P. C.; Chun, J.; Brinkmann, V.; Waeber, C. Analysis of sphingosine 1-phosphate receptors involved in constriction of isolated cerebral arteries with receptor null mice and pharmacological tools. *Br. J. Pharmacol.* **2008**, *153*, 140–147.
- (65) Gon, Y.; Wood, M. R.; Kiosses, W. B.; Jo, E.; Sanna, M. G.; Chun, J.; Rosen, H. SIP₃ receptor-induced reorganization of epithelial tight junctions compromises lung barrier integrity and is potentiated by TNF. *Proc. Natl. Acad. Sci. U.S.A.* **2005**, *102*, 9270–9275.
- (66) Buzard, D. J.; Thatté, J.; Lerner, M.; Edwards, J.; Jones, R. M. Recent progress in the development of selective SIP₁ receptor agonists for the treatment of inflammatory and autoimmune disorders. *Expert Opin. Ther. Pat.* **2008**, *18*, 1141–1159.
- (67) Brown, F. C. 4-Thiazolidinones. *Chem. Rev.* **1961**, *61*, 463–521.

- (68) Singh, S. P.; Parmar, S. S.; Raman, K.; Stenberg, V. I. Chemistry and Biological Activity of Thiazolidinones. *Chem. Rev.* **1981**, *81*, 175–203.
- (69) Bhargave, P. N.; Prakash, S.; Lakhan, R. Synthesis of 2-(4', 5'-Disubstituted-thiazol-2'-ylimino)-3-(*m*-methylphenyl)-5-methyl (or H) -4-thiazolidinones and Their Fungicidal Activity. *Indian J. Chem., Sect. B: Org. Chem. Incl. Med. Chem.* **1981**, *20*, 927–929.
- (70) Gruner, M.; Rehwald, M.; Eckert, K.; Gewald, K. New Synthesis of 2-Alkylthio-4-oxo-3,4-dihydro-quinazolines, 2-Alkylthioquinazolines, as well as Their Hetero Analogues. *Heterocycles* **2000**, *53*, 2363–2377.
- (71) Sedlak, M.; Hejtmankova, L.; Hanusek, J.; Machacek, V. Synthesis and ring transformation of substituted *S*-(1-phenylpyrrolidine-2-one-3-yl)isothiuronium salts to substituted 2-imino-5-[2-(phenylamine)ethyl]thiazolidin-4-ones. *J. Heterocycl. Chem.* **2002**, *39*, 1105–1107.
- (72) Blanchet, J.; Zhu, J. Reeve's synthesis of 2-imino-4-thiazolidinone from alkyl (aryl) trichloromethylcarbinol revisited, a three-component process from aldehyde, chloroform and thiourea. *Tetrahedron Lett.* **2004**, *45*, 4449–4452.
- (73) Gabillet, S.; Lecerclé, D.; Loreau, O.; Carboni, M.; Dézard, S.; Gomis, J.-M.; Taran, F. Phosphine-Catalysed Construction of Sulfur Heterocycles. *Org. Lett.* **2007**, *9*, 3925–3927.
- (74) Maly, R. Ueber Sulphydantoïn (Glycolylsulfoharnstoff). *Justus Liebigs Ann. Chem.* **1873**, *168*, 133–139.
- (75) Volhard, J. Ueber Glycolylsulfoharnstoff. *Justus Liebigs Ann. Chem.* **1873**, *166*, 383–384.
- (76) Meyer, P. J. Ueber substituierte Sulfohydantoïne. *Berichte Dtsch. Chem. Ges.* **1877**, *10*, 1965–1967.
- (77) Liebermann, C.; Lange, A. Ueber die Formeln der Sulphydantoïne. *Berichte Dtsch. Chem. Ges.* **1879**, *12*, 1588–1595.
- (78) Liebermann, C. Zur Constitution der Sulphydantoïne und Sulfur-ethane. *Ann. Chem.* **1881**, *207*, 121–167.
- (79) Steel, P. J.; Guard, J. A. M. Heterocyclic tautomerism. VI. A redetermination and reassignment of the structure of 2-aminothiazol-4(5*H*)-one. *Acta Crystallogr. Sect. C: Cryst. Struct. Commun.* **1994**, *50*, 1721–1723.
- (80) Ottanà, R.; Maccari, R.; Berreca, M. L.; Bruno, G.; Rotondo, A.; Rossi, A.; Chiricosta, G.; Paola, R. D.; Sautebin, L.; Cuzzocrea, S.; Vigorita, M. G. 5-Arylidene-2-imino-4-thiazolidinones: design and synthesis of novel anti-inflammatory agents. *Bioorg. Med. Chem.* **2005**, *13*, 4243–4252.
- (81) Klika, K. D.; Janovec, L.; Imrich, J.; Suchár, G.; Pavol, K.; Sillanpää, R.; Kalevi, P. Regioselective synthesis of 2-imino-1,3-thiazolidin-4-ones by treatment of *N*-(anthracen-9-yl)-*N'*-ethylthiourea with bromoacetic acid derivatives. *Eur. J. Org. Chem.* **2002**, 1248–1255.
- (82) Klika, K. D.; Valtamo, P.; Janovec, L.; Suchár, G.; Kristian, P.; Imrich, J.; Kivelä, H.; Alföldi, J.; Pihlaja, K. Regioselective syntheses, structural characterization, and electron ionization mass spectrometric behavior of regioisomeric 2,3-disubstituted 2-imino-1,3-thiazolidin-4-ones. *Rapid Commun. Mass Spectrom.* **2004**, *18*, 87–95.
- (83) Géci, I.; Valtamo, P.; Imrich, J.; Kivelä, H.; Kristian, P.; Pihlaja, K. Regiospecific Synthesis, Structure and Electron Ionization Mass Spectra of 1,3-Thiazolidine-4-ones Containing the Acridine Skeleton. *J. Heterocycl. Chem.* **2005**, *42*, 907–918.
- (84) Sahu, M.; Garnaik, B. K.; Behera, R. K. Influence of Substituents on the Synthesis of Thiazolidinones. *Indian J. Chem., Sect. B: Org. Chem. Incl. Med. Chem.* **1987**, *26*, 779–781.
- (85) Laurent, D. R. S.; Gao, Q.; Wu, D.; Serrano-Wu, M. H. Regioselective synthesis of 3-(heteroaryl)-iminothiazolidin-4-ones. *Tetrahedron Lett.* **2004**, *45*, 1907–1910.
- (86) Johnson, T. B. On the Molecular Rearrangement of Thiocyanacetanilides into Labile Pseudothiohydantoins and on the Molecular Rearrangement of the Later into Stable Isomers. *J. Am. Chem. Soc.* **1903**, *25*, 483–491.
- (87) Bolli, M.; Scherz, M.; Müller, C.; Mathys, M.; Lehmann, D. 5-(Benz-(*Z*)-ylidene)-thiazolidin-4-one derivatives as immunosuppressant agents. Patent WO2005054215, 2005.
- (88) Moghaddam, F. M.; Hojabri, L. A Novel Synthesis of Some 2-Imino-4-thiazolidinone Derivatives. *J. Heterocycl. Chem.* **2007**, *44*, 35–38.
- (89) Erol, S.; Dogan, I. Axially Chiral 2-Arylimino-3-aryl-thiazolidine-4-one Derivatives: Enantiomeric Separation and Determination of Racemization Barriers by Chiral HPLC. *J. Org. Chem.* **2007**, *72*, 2494–2500.
- (90) Clayden, J.; Moran, W. J.; Edwards, P. J.; LaPlante, S. R. The Challenge of Atropisomerism in Drug Discovery. *Angew. Chem., Int. Ed.* **2009**, *48*, 6398–6401.
- (91) Taylor, J. B.; Triggle, D. J. *Comprehensive Medicinal Chemistry II*. Elsevier: New York, 2007; Vol. 5, pp 133–165.
- (92) Jeong, E. J.; Liu, X.; Jia, X.; Chen, J.; Hu, M. Coupling of Conjugating Enzymes and Efflux Transporters: Impact on Bioavailability and Drug Interactions. *Curr. Drug Metab.* **2005**, *6*, 455–468.
- (93) Crosignani, S.; Bombrun, A.; Covini, D.; Maio, M.; Marin, D.; Quattropani, A.; Swinnen, D.; Simpson, D.; Sauer, W.; Francon, B.; Martin, T.; Cambet, Y.; Nichols, A.; Martinou, I.; Burgat-Charvillon, F.; Rivron, D.; Donini, C.; Schott, O.; Eligert, V.; Novo-Perez, L.; Vitte, P.-A.; Arrighi, J.-F. Discovery of a novel series of potent S1P₁ agonists. *Bioorg. Med. Chem. Lett.* **2010**, *20*, 1516–1519.
- (94) Piali, L.; Hess, P.; Kohl, C.; Nayler, O.; Bolli, M.; Steiner, B. S. 76. Selective S1P₁ Receptor Agonist ACT-128800 Rapidly and Reversibly Reduces Blood Lymphocyte Count. FOCIS 2009, San Francisco, June 11–14, 2009; p S153.
- (95) Brossard, P.; Hofmann, S.; Cavallaro, M.; Halabi, A.; Dingemanse, J. Entry-into-humans study with ACT-128800, a selective S1P₁ receptor agonist: tolerability, safety, pharmacokinetics, and pharmacodynamics. ASCPT 2009, Annual Meeting of the American Society for Clinical Pharmacology & Therapeutics, Washington, DC, March 18–21, 2009; pp S63–S64, PII-87.